DOE/NASA CONTRACTOR REPORT

DOE/NASA CR-161546

SOLAR ENERGY SYSTEM PERFORMANCE EVALUATION - SEASONAL REPORT FOR WORMSER, COLUMBIA, SOUTH CAROLINA

Prepared by

IBM Corporation
Federal Systems Division
150 Sparkman Drive
Huntsville, Alabama 35805

Under Contract NAS8-32036 with

National Aeronautics and Space Administration
George C. Marshall Space Flight Center, Alabama 35812

For the U. S. Department of Energy

(NASA-CR-161546) SOLAR ENERGY SYSTEM PERFORMANCE EVALUATION. SEASONAL REPORT FOR WORMSER, COLUMBIA, SOUTH CAROLINA Contractor Report, Jun. 1979 - May 1980 (IBM Federal Systems Div.) 110 p HC A06/MF A01 G3/44 28640

N80-31880

Unclas

U.S. Department of Energy

Solar Energy

TABLE OF CONTENTS

LIST OF FIGURES

LIST OF TABLES

1. FOREWORD

This Solar Energy System Performance Evaluation - Seasonal Report has been developed for the George C. Marshall Space Flight Center as a part of the Solar Heating and Cooling Development Program funded by the Department of Energy. The analysis contained in this document describes the technical performance of an Operational Test Site (OTS) functioning throughout a specified period of time which is typically one season. The objective of the analysis is to report the long term performance of the installed system and to make technical contributions to the definition of techniques and requirements for solar energy system design.

The contents of this document have been divided into the following topics of discussion:

- System Description
- Performance Assessment
- Operating Energy
- Energy Savings
- Maintenance
- Summary and Conclusions

Data used for the seasonal analyses of the Operational Test Site described in this document have been collected, processed and maintained under the OTS Development Program and have provided the major inputs used to perform the long-term technical assessment. This data is archived by the Marshall Space Flight Center for the Department of Energy.

The Seasonal Report document in conjunction with the Final Report for each Operational Test Site in the Development Program culminates the technical activities which began with the site selection and instrumentation system design in April 1976. The Final Report emphasizes the economic analysis of solar systems performance and features the payback performance based on life cycle costs for the same solar system in various geographic regions. Other documents specifically related to this system are References [1] through [5].*

*Numbers in brackets designate references found in Section 8.

2. SYSTEM DESCRIPTION

The Wormser solar energy site, located in Columbia, South Carolina, is comprised of four townhouse apartments. The solar collection system consists of flat-plate liquid collectors augmented by pyramidal reflectors, whose effective aperture varies from 280 to 740 square feet, that collect and store energy in a 2,500-gallon water tank. The transport fluid is water. In order to conform to the National Bureau of Standards Performance Evaluation Procedures, the gross collector array area is assumed to be equal to the solar window area which is 1,152 square feet. The window faces south at an angle of 30 degrees to the horizontal. The collectors themselves are located behind the window in the attic of two of the town houses and face south at an angle of 65 degrees to the horizontal. The pyramidal reflectors concentrate the solar energy on the collectors to produce a solar multiplication effect. Solar heated water is pumped in a loop between an internal heat exchanger within the 2,500-gallon storage tank and heat exchangers within four 120-gallon domestic hot water tanks that supply individual apartments with domestic hot water(DHW). An electric element in each domestic hot water tank supplies the necessary auxiliary energy to meet the hot water demand. Solar heated water is also supplied to a direct solar-to-air heat exchanger or to a multi-functional heat pump (contains both liquid-to-air and air-to-air modes) that supplies space heating energy to each apartment. Freeze protection for the collectors is provided through the location of the collectors inside the attic. The system is shown schematically in Figure 2-1 and has six modes of operation. The sensor designations in Figure 2-1 are in accordance with NBSIR-76-1137 [6]. The measurement symbol prefixes: W, T, EP, I and F represent respectively: flow rate, temperature, electric power, insolation, and fossil fuel consumption. Figure 2-2 is a pictorial view of one of the two townhouse apartments that contains a collector array.

Mode 1 - Collector-to-Storage: This mode is entered when the difference in temperature between the collector outlet and a temperature representative of storage is 15 degrees or higher. The thermal transfer fluid is

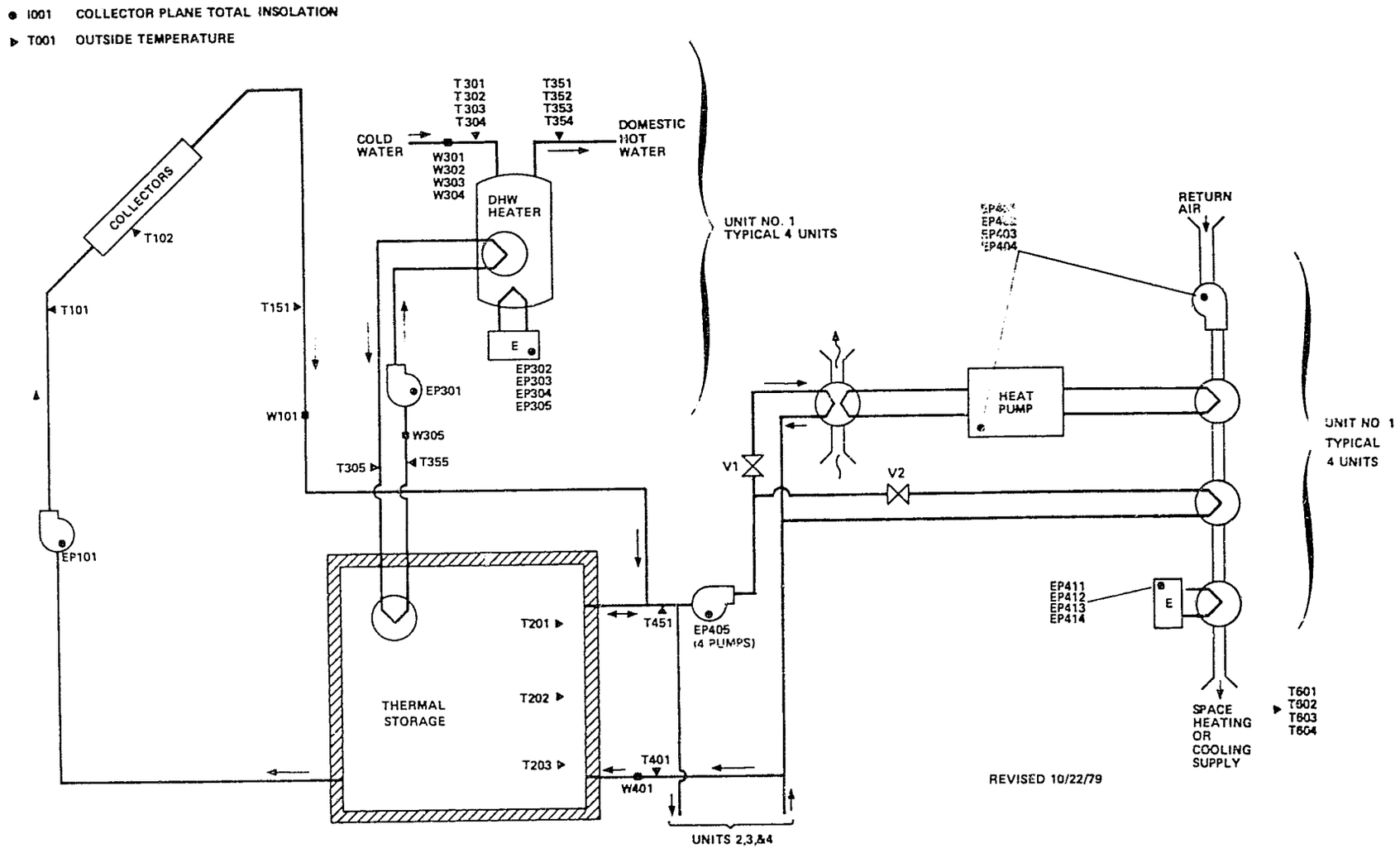

Figure 2-1 Wormser Scientific Corporation Solar Energy System Schematic

Figure 2-2 Wormser Pictorial and Collector Array Detail

circulated through the collectors using circulation pump P1 to thermal storage and then recirculated to the collectors. Circulation continues in this mode until the difference between the collector outlet and storage is less than 5 degrees.

Mode 2 - Storage-to-Space Heating (Direct Solar Only): This mode is entered when there is a demand for space heating and the temperature in storage is greater than 85°F. Water from storage is circulated through the direct solar-to-air heat exchanger using pumps P2 through P6, and then returned to storage. The heat pump fan transfers energy to the building. Circulation continues in this mode until thermal storage temperature drops below 85°F or the demand for space heating ceases.

Mode 3 - Collector/Water-Air Heat Pump Heating Mode: This mode is entered when there is a demand for space heating and the temperature in storage is lower than 85°F. This mode allows energy to be transferred from storage or direct from the collectors (bypassing storage). Water from storage or collectors is circulated through heat pumps operating in liquid-to-air mode using pumps P2 through P6. The heat pump fan transfers energy to the building. Stage 2 of the space heating thermostat activates the first stage of auxiliary electric heat strips in the supply duct to supplement solar energy to satisfy the demand for heating. This condition occurs during any heating mode. Circulation continues in this mode until the temperature of the solar heated water drops below 50°F or the demand for space heating ceases.

Mode 4 - Air-to-Air Heat Pump Heating Mode: When solar energy for space heating is not available, i.e., the storage temperature is less than 50°F, stage 1 of the space heating thermostat activates the heat pump operating in the air-to-air mode to supply the required energy to satisfy the demand for heating. If the outside temperature drops below 20°F, the second stage of the heat strips is activated and the heat pump is deactivated. Space heating continues in this mode until the demand ceases.

Mode 5 - Conventional Cooling: A manual changeover of the house thermostat at the end of the heating season initiates this mode. The heat pump functions in the air-to-air mode providing air conditioning. This mode is auxiliary only and has no solar involvement.

Mode 6 - Hot Water Preheating: This mode is entered when the temperature in the return lines of the last storage tank is greater than 10°F below the solar storage tank temperature. Water from the solar tank is circulated to all four domestic hot water (DHW) tanks and returned. The electric elements in the domestic hot water tanks supply auxiliary energy to meet the domestic hot water demand. Circulation continues in this mode until the temperature in the return lines is less than 2 degrees below the solar storage tank.

These modes in themselves are not exclusive since the system can be performing more than one function at any given time. This is due to the independence of the differential controller for the collector pump, the controller for the space heating subsystem and the differential controller for the domestic hot water subsystem temperature.

2.1 Typical System Operation

Curves depicting typical system operation on a cool bright day (February 26, 1980) are presented in Figures 2.1-1 (a) through 2.1-1 (e).

Figure 2.1-1 (a) shows the insolation on the collector array and the period when the array was operating (shaded area). On this particular day collector array initiation first occurred at 8:37 AM, then shut off when temperatures dropped below the cutoff set points. The second collector array initiations occurred at 9:30 AM and collector array operation continued until 1612 hours when it was shut down for the day. The insolation reached a peak value of 310 Btu/Hr-Ft^2 at 12:26 PM.

Figures 2.1-1 (b), 2.1-1 (c), and 2.1-1 (d) show typical collector array temperatures during the day. During the early morning hours the collector array outlet temperature (T151), the collector array inlet temperature (T101) and the collector absorber plate temperature (T103) continued to decay from the temperatures achieved during the previous day's collection. As the sun started to rise at approximately 7:14 AM, T103 began to rise rapidly and reached 76°F before the system turned on prematurely at 8:37 AM. When conditions again warranted collector array initiation at 9:30 AM, T103 dropped from a peak value of 103°F to a stable temperature of 90°F. The absorber temperature rose slowly throughout the day reaching a peak value of 115°F at 2:47 PM. It should be noted that T103 is not the control sensor that governs system operation. However, the absorber temperature (T103) is in close proximity to the collector control sensor and as such provides an indication of collector plate temperatures in the vicinity of the control sensor. The actual system controls are set up such that a differential temperature of 15°F between the collector and storage is required before collected energy can be delivered to storage. The array initiating differential temperature at 9:30 AM was approximately 14°F which was close to the expected value and indicates the control system operated properly to initiate collector turn-on.

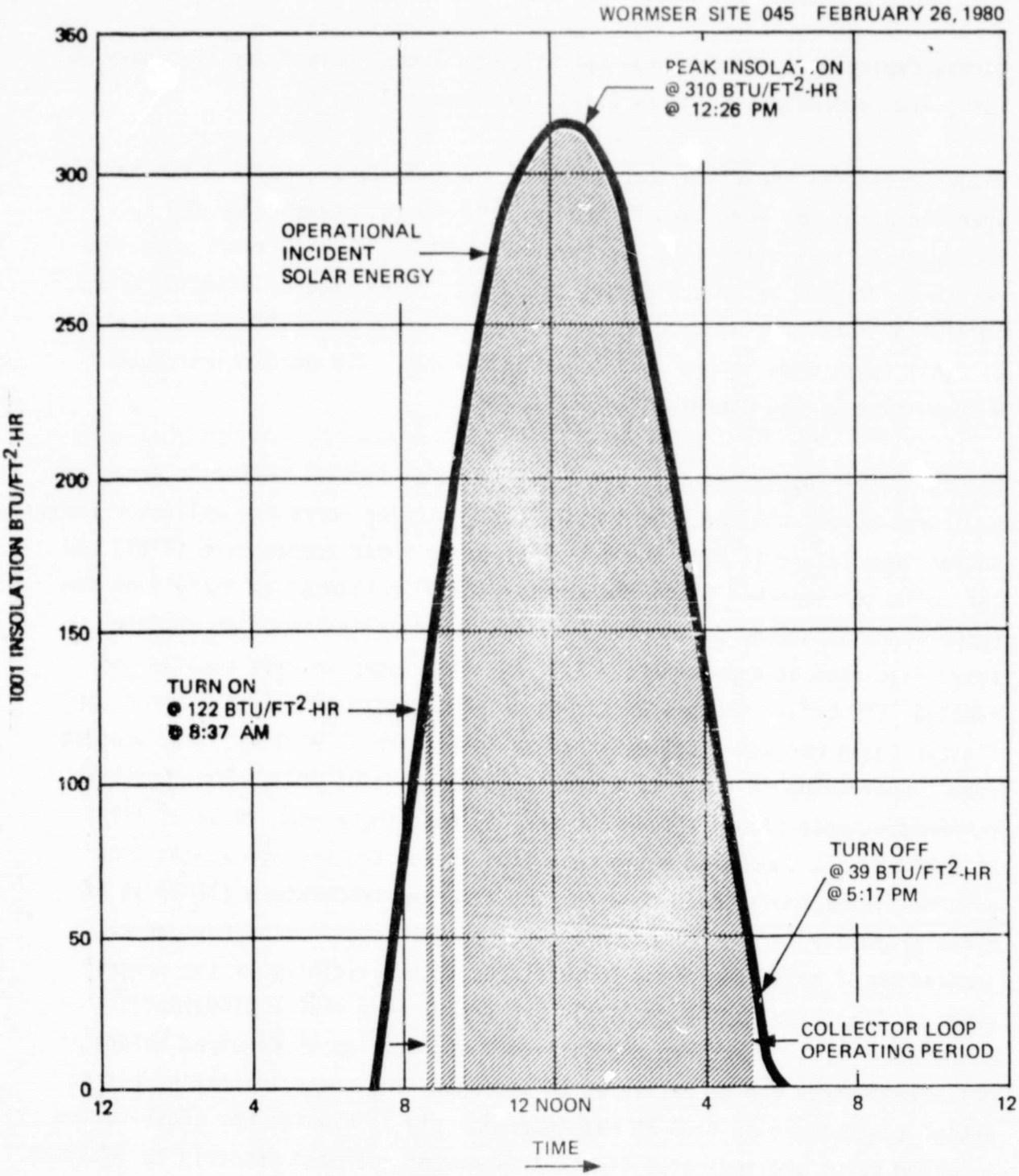

Figure 2.1-1(a) Solar Insolation Vs. Time of Day

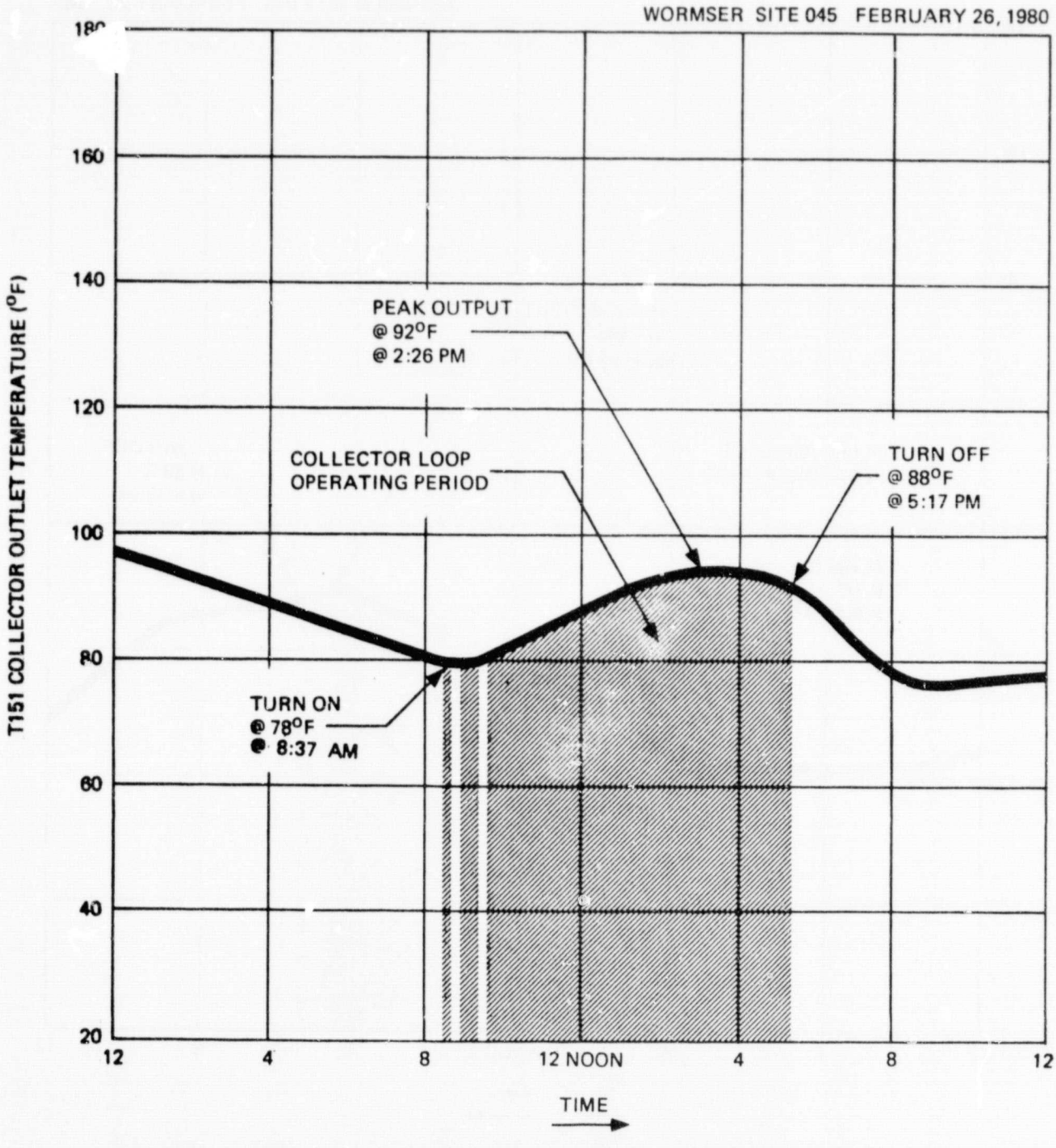

Figure 2.1-1(b) Collector Outlet Temperature Vs. Time of Day

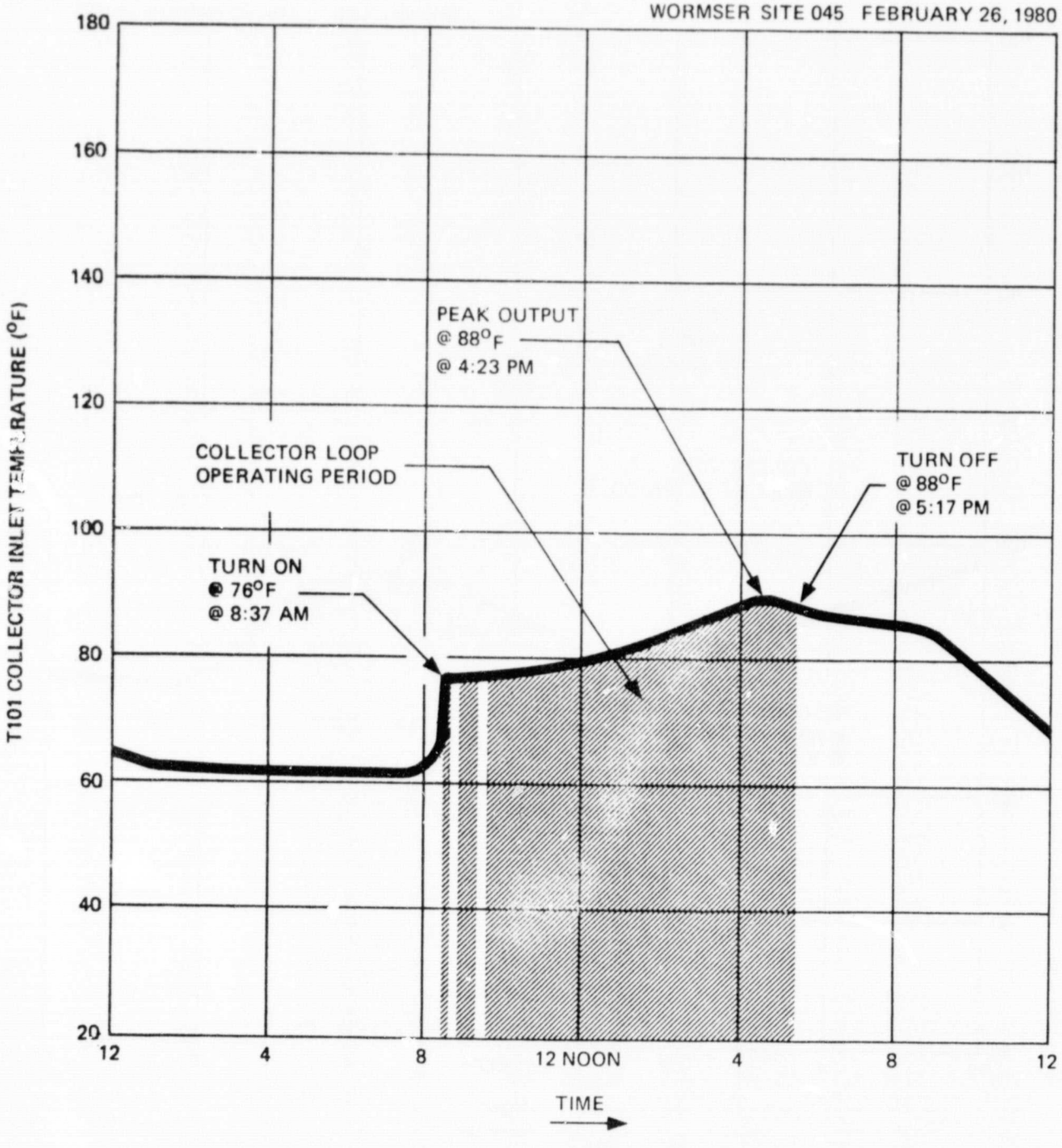

Figure 2.1-1(c) Collector Inlet Temperature Vs. Time of Day

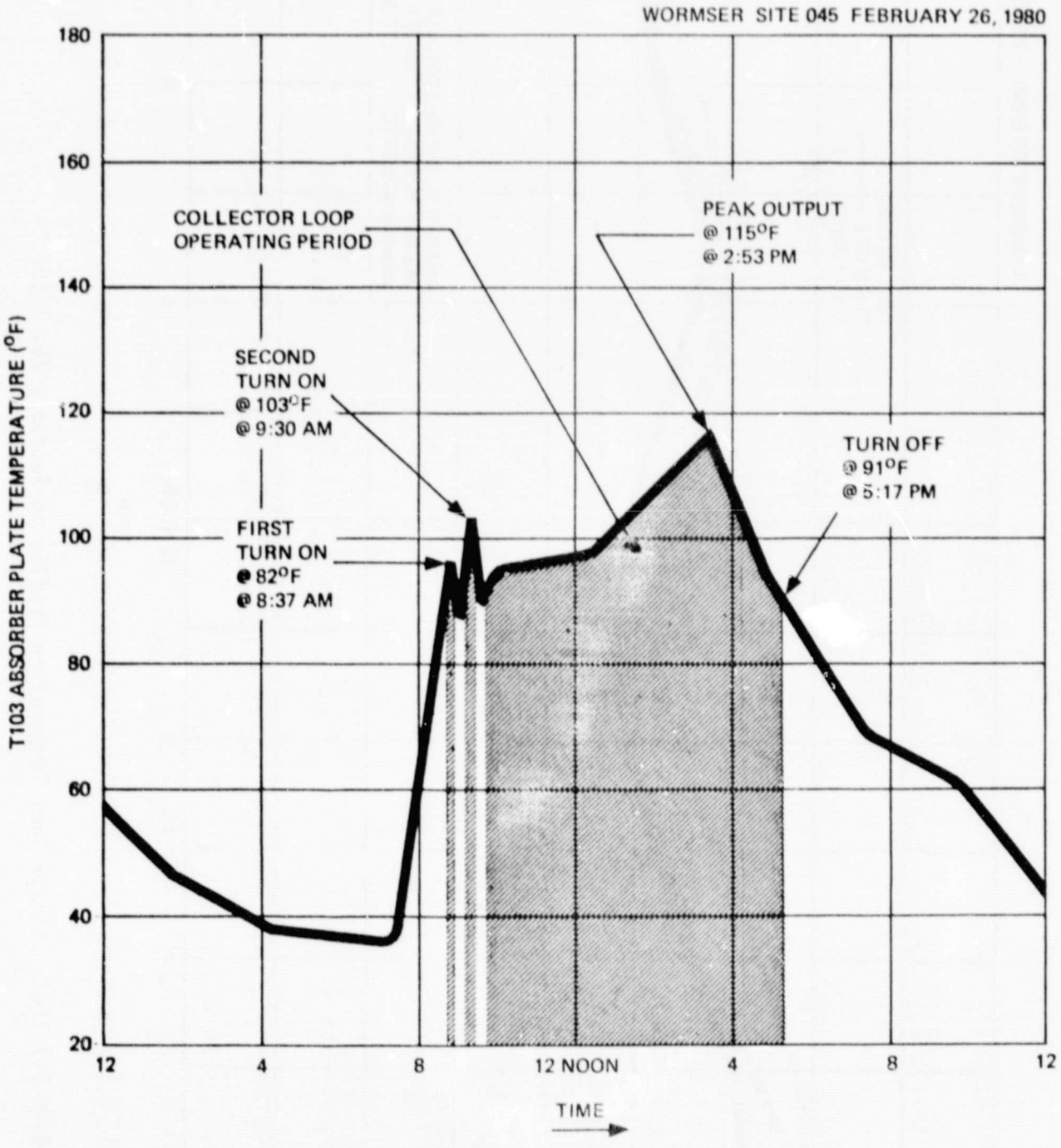

Figure 2.1-1(d) Absorber Plate Temperature Vs. Time of Day

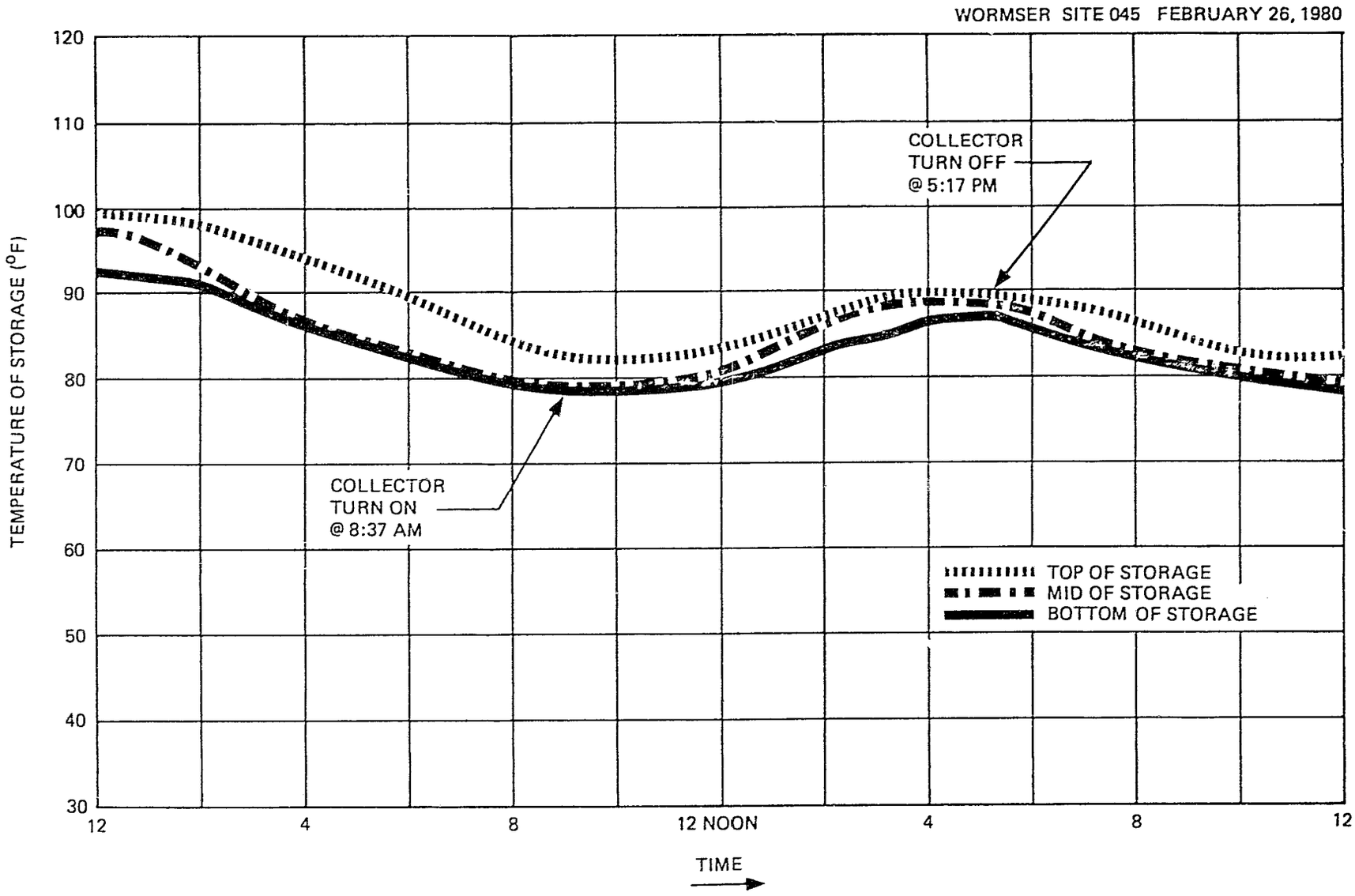

Figure 2.1-1(e) Storage Tank Temperature Profile on February 26, 1980

The collector outlet temperature (T151) rose to a maximum value of 92°F at 2:26 PM while the collector inlet temperature maximum of 88°F occurred at 4:23 PM. The highest collector inlet to outlet differential temperature achieved was 8.6°F; and, correspondingly the highest collector outlet to storage bottom temperature achieved was 8.6°F both of which occurred at 12:37 PM.

Collector array turn-off occurred at 5:17 PM when the collector inlet to outlet temperature differential reduced below 0.5°F. The absorber to storage bottom differential was 4°F. Again these temperature differentials are slightly below the design temperature differential of 5°F; however, no control instabilities occurred. These operating temperature constraints are mentioned to make the reader aware that monitoring instrumentation and control sensors do not have direct correlation, but monitoring instrumentation can provide sufficient gross data to determine if each operational mode is functioning within a reasonable range of control temperature sensor limits.

Figure 2.1-1 (e) shows the temperature profile of the 2,500 gallon liquid storage tank. During the early morning hours all space heating demands were satisfied with stored solar energy until 4:00 AM when supplemental auxiliary energy was required when the solar storage tank temperature dropped below 85°F. The supplemental auxiliary energy initiated was the 1st stage heat strips. Normally the space heating subsystem would switch to the heat pump solar Mode 3. However, this space heating control system at times switched to a solar plus heat strip mode which is undesirable. The solar storage subsystem is designed to supply all space heating energy requirements down to a storage temperature of 85°F which is actually what happened. The solar storage tank temperatures continued to decay as energy was removed. Solar and auxiliary energy contributions to space heating continued throughout the remainder of the day. After the collector array began operating normally at 9:30 AM, the storage tank began to warm up and continued to do so until 2:26 PM. The maximum storage temperature achieved was 92°F. For the remainder of the day, stored solar energy was able to satisfy most of the space heating demand.

2.2 System Operating Sequence

Figure 2.2-1 presents bar charts showing typical system operating sequences for February 26, 1980. This data correlates with the curves presented in Figures 2.1-1 (a) through (e)

There are two interesting observations that can be made from Figure 2.2-1. First is the high DHW usage. The high DHW usage is typical of this solar-energy system. Indeed, most of the overall DHW solar subsystem savings results from operation of the DHW solar subsystem. Approximately 45 percent of the solar energy collected was delivered to the DHW subsystem. Solar energy contributed to the DHW demand throughout the day. Auxiliary electric energy was required when large, hot water heating demands occurred. However, most of the DHW tank and piping losses were replenished by solar energy.

The second observation relates to the use of space heating auxiliary energy. Stored solar energy was sufficient to meet the entire space heating demand until 4:00 AM when the storage tank temperature decayed below 85°F. The space heating control system is designed to switch to heat pump - solar mode 3 for storage tank temperatures below 85°F. However, the control system apparently operated incorrectly this particular day, reverting to a solar plus heat strip submode which was very detrimental to solar energy savings. This type of operation occurred too often during the winter months. At the time of solar collection initiation, storage tank temperatures were still above the threshold temperature of 50°F necessary for solar energy space heating utilization. Solar and auxiliary energy met the load demands throughout the remainder of the day. The auxiliary consumption associated with each apartment is indicated by the numbers above the bar along with the time period that the consumption occurred. Generally, Apartment Number 4 operated most of the time in this undesirable submode.

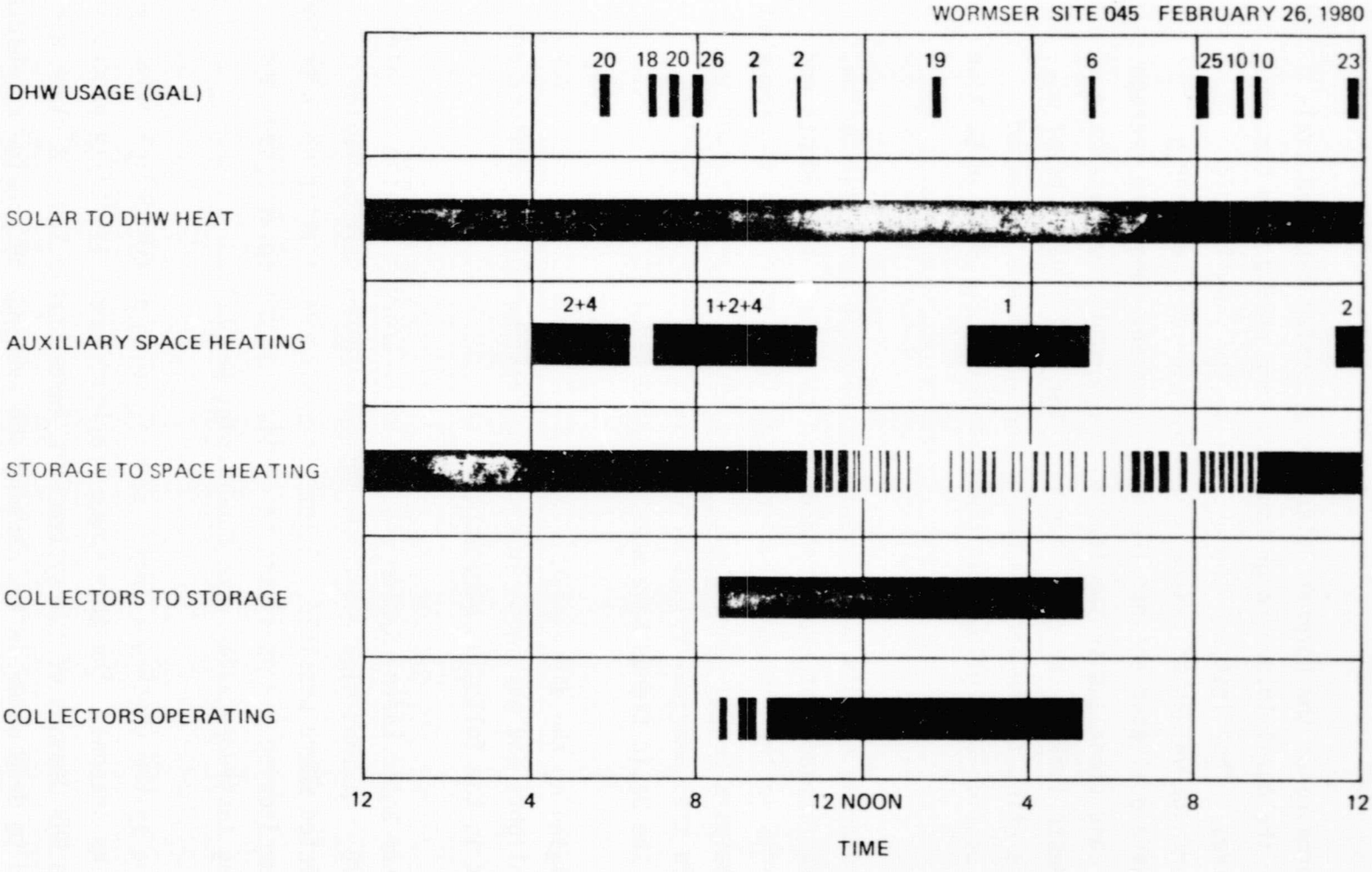

Figure 2.2-1 Typical System Operating Sequence

3. PERFORMANCE ASSESSMENT

The performance of the Wormser Solar Energy System has been evaluated for the April 1979 through May 1980 time period from two perspectives. The first was the overall system view in which the performance values of system solar fraction and net energy savings were evaluated against the prevailing and long-term average climatic conditions and system loads. The second view presents a more in-depth look at the performance of the individual subsystems. Details relating to the performance of the system are presented first in Section 3.1 followed by the subsystem assessment in Section 3.2.

For the purposes of this solar energy system performance evaluation, monthly performance data were regenerated to reflect refinements and improvements in the system performance equations that were incorporated as the analysis period progressed. These modifications resulted in changes in the numerical values of some of the performance factors. However, the basic trends have not been affected.

Before beginning the discussion of actual solar energy system performance some highlights and pertinent information relating to site history are presented in the following paragraphs.

The Wormser Solar Energy System was initially brought on line in late March 1978. At that time all known system problems were addressed and corrected where possible. After the system was started up, a period of data monitoring was initiated to verify that the solar system and monitoring instrumentation were functioning properly.

During the system check-out phase, several solar system deficiencies were found to be present. The town house apartments were initially unoccupied. Thus, the DHW demands of the system were unreasonably low. A clock was installed to draw water in the morning and evenings to provide a measure of performance for the DHW subsystems.

Initial investigation revealed that the storage tank and connecting pipes were uninsulated. The solar system remained in this condition until October 30, 1978 when the storage tanks and transport piping were insulated and a failed storage tank repaired.

The collector subsystem was inoperative until November 2, 1978 when air was bled from the collector piping. The collectors have operated as designed since this time.

In late November, solar space heating liquid flow was initiated. It was immediately evident that the present flow meter could not accurately measure single apartment liquid flow. The flow meter excitation voltage was raised and the resulting signal-to-noise ratio permitted accurate measurement of solar storage tank flow.

Unit No. 3 was occupied in mid-December 1978 and hot water consumption using automatic control removed.

Unit #2 heat pump was repaired between January 3-5, 1979. The apartment was occupied shortly after this date.

The DHW controller failed February 1, 1979 and no solar energy flow to the DHW tanks was indicated until March 22, 1979 when the problems with the subsystem were resolved.

DHW subsystem operation was improved in June 1979 by adjustment of the DHW controller set points. The solar contribution to this subsystem improved substantially since that event.

Apartments No. 1 and 4 were occupied in June 1979. After this time, the solar system heating and hot water demands were representative of that which occurs in a four Town-house apartment complex.

Analysis of data prior to June 1979, indicated that accurate determination of space heating load could not be achieved with the present instrumentation. Power meters EP401 through EP404 measured heat pump power, circulation fan power and heat strip power. Separation of the heat strip power to new wattmeters was suggested. On November 9, 1979, wattmeters EP411 and EP414, auxiliary power to Apartments 1 and 4 respectively, were correctly wired and normal operation verified. On December 12, 1979, wattmeters EP412 and EP413, auxiliary heat strip power to apartments 2 and 3, were wired and normal operation verified. After this date, accurate space heating demand could be measured. Prior to this time uncertainties exist in the space heating demand computations and should be realized when observing the performance factor results for prior months.

Because of the solar system deficiencies throughout the monitoring period March 1978 to May 1980, only the period June 1979 through May 1980 is considered representative of proper solar energy system performance. This seasonal report is based on the solar system performance during this period.

3.1 System Performance

This Seasonal Report provides a system performance evaluation summary of the operation of the Wormser Solar Energy System located in Columbia, South Carolina. This analysis was conducted by evaluation of measured system performance against the expected performance with long-term average climatic conditions. The performance of the system is evaluated by calculating a set of primary performance factors which are based on those proposed in the intergovernmental agency report, "Thermal Data Requirements and Performance Evaluation Procedures for the National Solar Heating and Cooling Demonstration Program" [6]. The performance of the major subsystems is also evaluated in subsequent sections of this report.

The measurement data were collected for the period March 1978 through May 1980. However, the Seasonal Report is based on data collected between June 1979 and May 1980. This period represents the best indication of solar system performance. Before this evaluation period, the solar system was either inactive or not configured as designed. System performance data were provided through an IBM developed Central Data Processing System (CDPS) [7] consisting of a remote Site Data Acquisition System (SDAS), telephone data transmission lines and couplers, an IBM System 7 computer for data management, and an IBM System 370/145 computer for data processing. The CDPS supports the collection and analysis of solar data acquired from instrumented systems located throughout the country. These data are processed daily and summarized into monthly performance formats which form a common basis for comparative system evaluation. These monthly summaries are the basis of the evaluation and data given in this report.

The solar energy system performance summarized in this section can be viewed as the dependent response of the system to certain primary inputs. This relationship is illustrated in Figure 3.1-1. The primary inputs are the incident solar energy, the outdoor ambient temperature and the system load. The dependent responses of the system are the system solar fraction and the total energy savings. Both the input and output definitions are as follows:

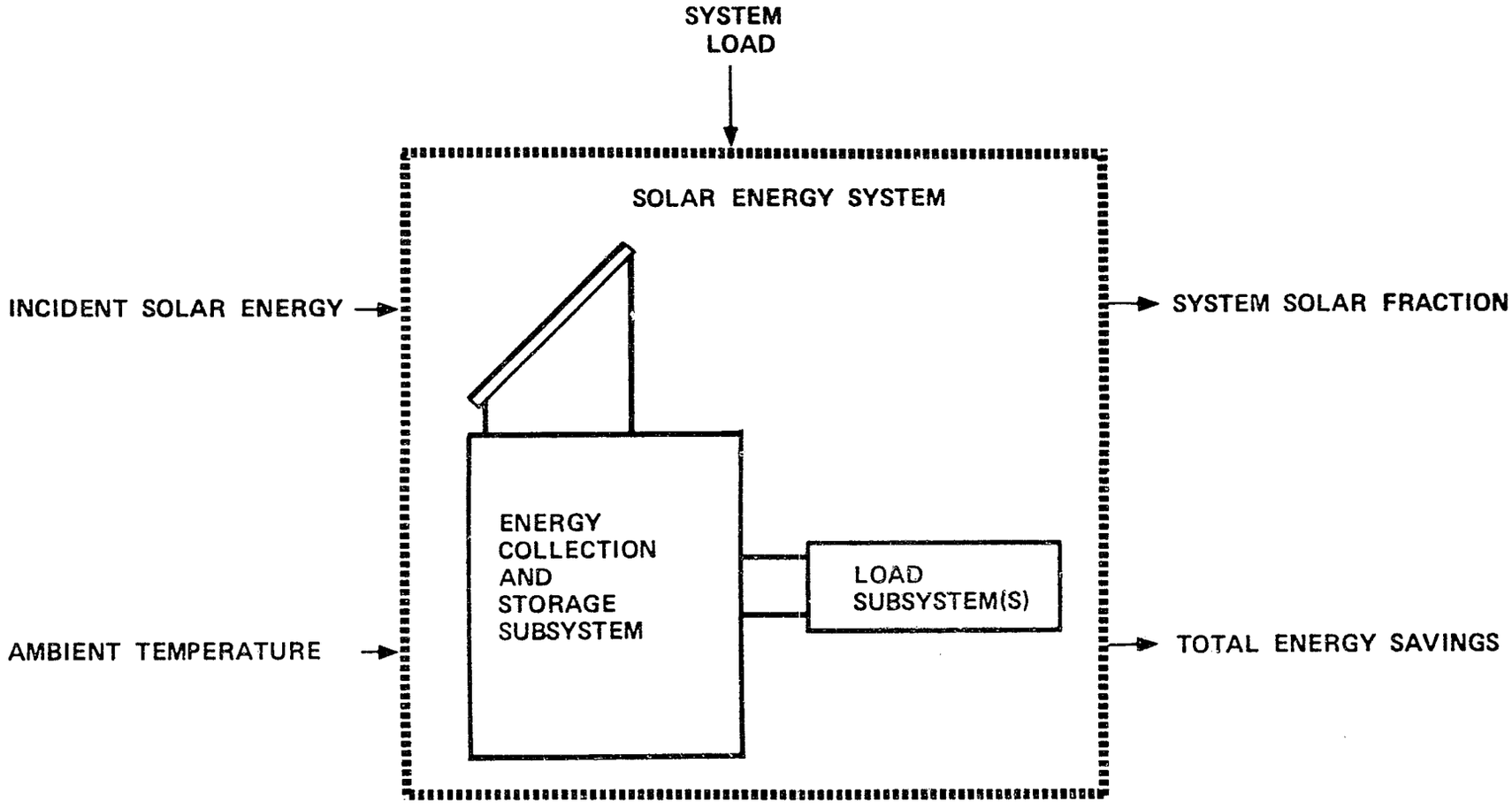

Figure 3.1-1 Solar Energy System Evaluation Block Diagram

Inputs

- Incident solar energy - The total solar energy incident on the collector array and available for collection.

- Ambient temperature - The temperature of the external environment which affects both the energy that can be collected and the energy demand.

- System load - The loads that the system is designed to meet, which are affected by the life style of the user (space heating/cooling, domestic hot water, etc., as applicable).

Outputs

- System solar fraction - The ratio of solar energy applied to the system loads to total energy (solar plus auxiliary energy) required by the loads.

- Total energy savings - The quantity of auxiliary energy (electrical or fossil) displaced by solar energy.

The monthly values of the inputs and outputs for the total operational period are shown in Table 3.1-1, the System Performance Summary. Comparative long-term average values of daily incident solar energy, and outdoor ambient temperature are given for reference purposes. The long-term data are taken from Reference 1 of Appendix C. Generally the solar energy system is designed to supply an amount of energy that results in a desired value of system solar fraction while operating under climatic conditions that are defined by the long-term average value of daily incident solar energy and outdoor ambient temperature. If the actual

TABLE 3.1-1

SYSTEM PERFORMANCE SUMMARY

WORMSER

Month	Daily Incident Solar Energy Per Unit Area (30° Tilt) (Btu/Ft²)		Ambient Temperature (°F)		System Load - Measured (Million Btu)	Solar Fraction (Percent)			Total Energy Savings Fossil Equivalent At Source (Million Btu)	Total Energy Savings Fossil Equivalent At Source After Elimination of Solar Plus Heat Strip Mode (Million Btu)
						Measured	Expected			
	Measured	Long-Term Average	Measured	Long-Term Average			Mod 1	Mod 2		
Jun 79	1,556	1,763	75	79	1.18	52	32	70	2.89	2.89
Jul 79	1,451	1,698	78	81	3.49	38	21	58	3.78	3.78
Aug 79	1,722	1,677	80	80	3.96	49	26	67	7.12	7.12
Sep 79	1,098	1,570	73	75	5.10	30	30	51	4.03	4.03
Oct 79	1,607	1,520	64	64	6.45	41	28	46	7.17	7.17
Nov 79	1,195	1,305	57	54	10.36	49	44	51	5.17	5.83
Dec 79	995	1,068	48	46	19.88	31	29	31	-0.17	5.00
Jan 80	697	1,084	44	45	22.36	16	17	15	-4.00	12.30
Feb 80	1,395	1,313	43	48	23.87	34	23	32	-16.50	-3.98
Mar 80	1,173	1,556	51	54	17.89	33	20	38	-8.20	0.10
Apr 80	1,657	1,789	64	64	7.52	40	16	52	5.23	5.25
May 80	1,628	1,781	71	72	5.83	42	23	66	8.20	8.20
Total	--	--	--	--	127.69	--	--	--	14.72	57.69
Average	1,348	1,510	62	64	10.66	33*	25	33	1.23	4.81

*Measured solar fraction is weighted by the system load.

climatic conditions are close to the long-term average values, there is little adverse impact on the system's ability to meet design goals. This is an important factor in evaluating system performance and is the reason the long-term average values are given. The data reported in the following paragraphs are taken from Table 3.1-1.

At the Wormser site for the 12 month report period, the long-term daily incident solar energy in the plane of the collector is estimated to be 1,510 Btu/Ft^2. The average daily measured value was 1,348 Btu/Ft^2 which is about eleven percent below the long-term value. On a monthly basis, January of 1980 was the worst month with an average daily measured value of incident solar energy 36 percent below the long-term average daily value. August 1979 was the best month with an average daily measured value three percent above the long-term average daily value. On a long-term basis the good and bad months should average out so that the long-term average performance should not be adversely influence by small differences between measured and long-term average incident solar energy.

The outdoor ambient temperature influences the operation of the solar energy system in two important ways. First the operating point of the collectors and consequently the collector efficiency or energy gain is determined by the difference in the outdoor ambient temperature and the collector inlet temperature. Secondly the load is influenced by the outdoor ambient temperature. The measured average daily ambient temperature for the period from April 1979 through May 1980 was 62°F at the Wormser site. This compares favorably with the long-term value of 64°F. Thus, the actual heating load during the reporting period should be close to the long-term averages.

It is interesting to note the strong influence that the local weather conditions had on the measured solar fraction. For example, the measured average outdoor ambient temperature in January 1980 was one degree below the long-term average, and in February 1980 it was five degrees below the long-term average. In January the measured insolation was 36 percent below the long-term average and the measured solar fraction was 16 percent. However, in February the measured insolation was 6 percent above the long-term average and the measured solar fraction was 34 percent. In March 1980 the measured insolation was 25 percent below the long-term average, and the measured average outdoor ambient temperature of 51°F was three degrees below the long-term average and the measured solar fraction was 33 percent. This is exactly what would be expected because, even though the insolation was low, the measured average outdoor ambient temperature for March was 8°F above that noted for the January-February time period. These observations serve to reinforce the earlier statement concerning the impact of prevailing weather conditions on the performance of a solar energy system.

The system load has an important affect on the system solar fraction and the total energy savings. If the load is small and sufficient energy is available from the collectors, the system solar fraction can be expected to be large. However, the total energy savings will be less than under more nominal load conditions. This is illustrated by comparing the performance of the system during the summer (June, July and August) and winter (December, January and February) months. During the summer the space heating load was negligible and the system was used primarily to support the hot water load. On the other hand, the space heating loads during the winter months were very near the long-term expected values. As a result the system solar fraction was higher in the summer months and lower in the winter months, however the summer energy savings tended to be smaller than winter savings.

The system savings were greatly affected by two factors: the inadvertent operation of the space heating system in a solar plus heat strip mode and the high water consumption during all months. The inadvertent operation of the heat strips required 12.89 million Btu of electrical energy and the equivalent cost at the source of energy generation would have been 42.97 million Btu. Thus, a severe penalty is incurred (four times the actual total possible energy savings) because the space heating subsystem operated

in a less efficient solar plus heat strip mode rather than the heat pump - solar mode 3 in winter months when the heating demand was high. Secondly, the high hot water demand resulted in reasonable solar fractions in summer months when large quantities of solar energy is available and low solar fractions in winter months when the space heating demand requirements were high.

Also presented in Table 3.1-1 are the measured and expected values of system solar fraction where system solar fraction is the ratio of solar energy applied to system loads to the total energy (solar plus auxiliary) applied to the loads. The table contains two expected values. The first expected value was derived using an assumed system model (Mod 1) that closely approximates this particular system (i.e., variable collector area). The second expected value was derived assuming that the window area consisted entirely of collector absorbers of the type used in this system with a plexiglass covering. The expected values have been derived from a modified f-Chart analysis which uses measured weather and subsystem loads as inputs (f-Chart is the designation of a procedure that was developed by the Solar Energy Laboratory, University of Wisconsin, Madison, for modeling and designing solar energy systems [11]). The model used in the analysis is based on manufacturers' data and other known system parameters. The basis for the model is a set of empirical correlations developed for liquid and air solar energy systems that are presented in graphical and equation form and referred to as the f-Charts, where 'f' is a designator for the system solar fraction. The output of the f-Chart procedure is the expected system solar fraction. The measured value of system solar fraction was computed from measurements, obtained through the instrumentation system, of the energy transfers that took place within the solar energy system. These represent the actual performance of the system installed at the site.

The measured value of system solar fraction can generally be compared with the expected value so long as the assumptions which are implicit in the f-Chart procedure reasonably apply to the system being analyzed. The complexity of this system with its variable collector area does not fit to the f-Chart model. However, applying this procedure may provide some insight as to how the system actually performed with respect to a more standard

application such as shown in the Mod 2 column in Table 3.1-1. As shown in Table 3.1-1, the measured system solar fraction of 33 percent was higher than the expected value of 25 percent generated by the modified f-Chart program assuming Mod 1. Although this variation is substantial, it must be realized that f-Chart prediction model is not suited to the type of system design used at Wormser. As can be seen, the winter month variations are generally smaller for either Mod 1 or 2. This result can be attributed to the fact that the effective collector area is close to the solar window area and, as such, the system performance for either model approaches the actual solar system situation. On the other hand, the summer performance of Mod 1 is considerably lower than the actual measured performance while the performance of Mod 2 is higher. The performance of Mod 2 in summer months can be expected because the collector area (solar window) is considerably larger than the collector effective area for those months. Thus, the f-Chart method of predicting the summer mode of operation does not result in good comparisons. It is possible that the large energy losses associated with operation of this subsystem have not been taken into account properly. However, even though the prediction models do not fit the solar energy system perfectly, the overall value of the f-Chart analysis tool should not be underestimated. The effect of the solar system on these factors associated with the Wormser site would require a more sophisticated analysis model than f-Chart.

The total energy savings is the most important performance parameter for the solar energy system because the fundamental purpose of the system is to replace expensive conventional energy sources with less expensive solar energy. In practical consideration, the system must save enough energy to cover both the cost of its own operation and to repay the initial investment for the system. In terms of the technical analysis presented in this report the net total energy savings should be a significant positive figure. The total computed energy savings for Wormser Solar Energy System if the undesirable solar plus heat strip mode had been eliminated was 14.72 million Btu, or 4313 kWh of electricity. This is equivalent to approximately 2.5 barrels of oil. This amount of savings is peculiar in view of the 33 percent solar fraction of the measured load achieved by the system. This discrepancy can be directly attributed to operating the system in the undesirable solar plus heat strip mode as opposed to

the heat pump solar mode. In addition, at Wormser site there were a significant amount of uncontrolled (and hence unmeasured) inputs of solar energy into the building. These uncontrolled inputs of solar energy came primarily from transport losses and tended to reduce the overall heating load, which in turn tended to increase real savings. This situation is addressed in more detail in the appropriate sections that follow.

3.2 Subsystem Performance

The Wormser Solar Energy Installation may be divided into four subsystems:

1. Collector array
2. Storage
3. Hot water
4. Space heating

Each subsystem has been evaluated by the techniques defined in Section 3 and is numerically analyzed each month for the monthly performance assessment. This section presents the results of integrating the monthly data available on the four subsystems for the period April 1979 through May 1980.

3.2.1 Collector Array Subsystem

The Wormser collector array consists of twenty-four on-site constructed flat-plate liquid collectors all connected in parallel. These collectors are copper roll bond type with a one-quarter inch plexi-glass glazing. The collectors are constructed in wooden boxes that contain six inches of fiber-glass backing. The absorber plate which is painted with black paint is open to the attic of the building. Solar energy is concentrated on the absorber using pyramidal reflectors to achieve a solar multiplication factor. The collector array arrangement is shown pictorially in Figure 3.2.1-1 (a). Details of the collector array liquid flow paths are shown in Figure 3.2.1-1 (b). The collector subsystem analysis and data are given in the following paragraphs.

Collector array performance is described by the collector array efficiency. This is the ratio of collected solar energy to incident solar energy, a value always less than unity because of collector losses. The incident solar energy may be viewed from two perspectives. The first assumes that all available solar energy incident on the collectors must be used in determining collector array efficiency. The efficiency is then expressed by the equation:

$$\eta_c = Q_s/Q_i \qquad (1)$$

where η_c = Collector array efficiency

Q_s = Collected solar energy

Q_i = Incident solar energy

The efficiency determined in this manner includes the operation of the control system. For example, solar energy can be available at the collector, but the collector absorber plate temperature may be below the minimum control temperature set point for collector loop operation, thus the energy is not collected. The monthly efficiency by this method is listed in the column entitled "Collector Array Efficiency" in Table 3.2.1-1.

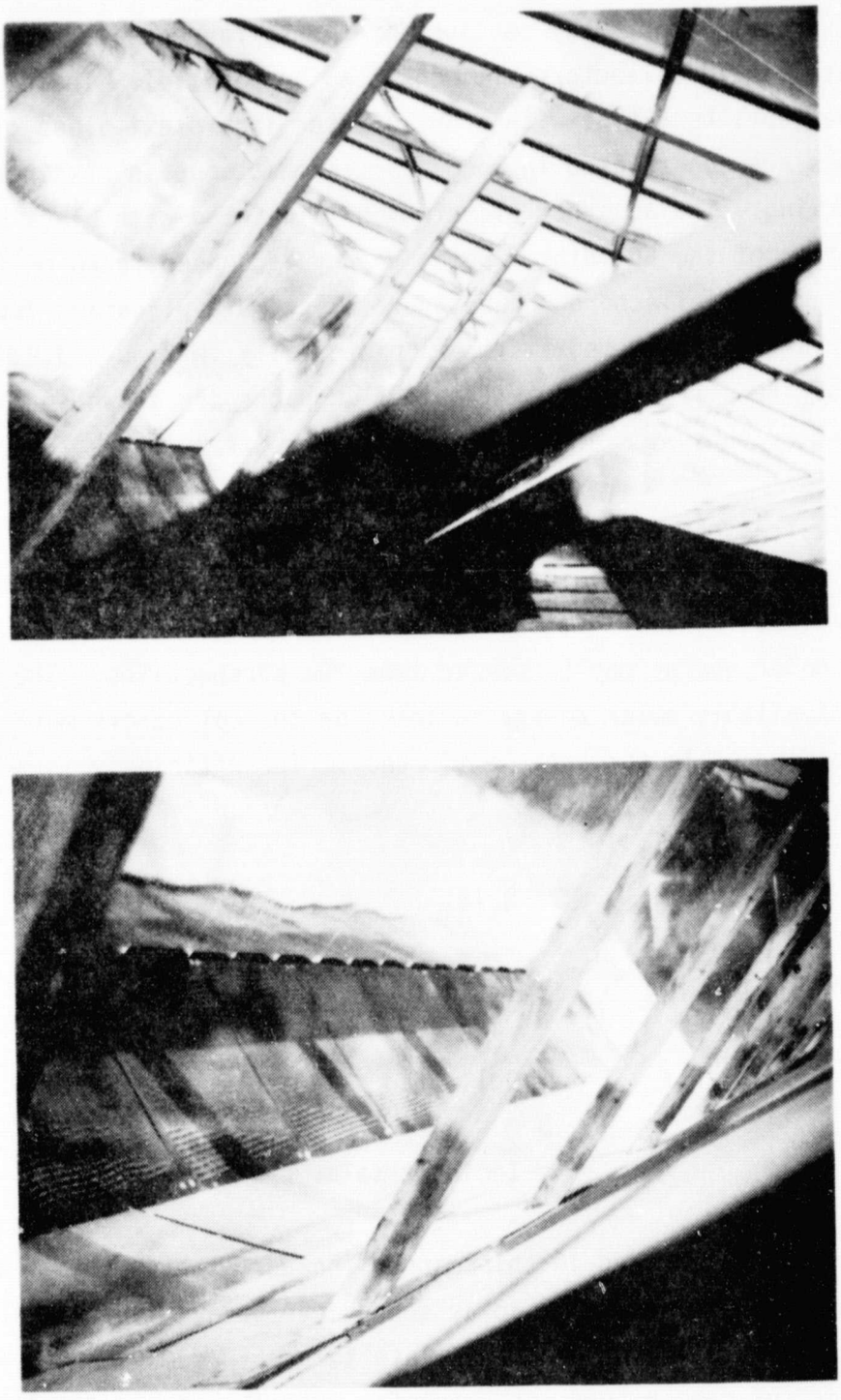

Figure 3.2.1-1(a) Collector Array Arrangement

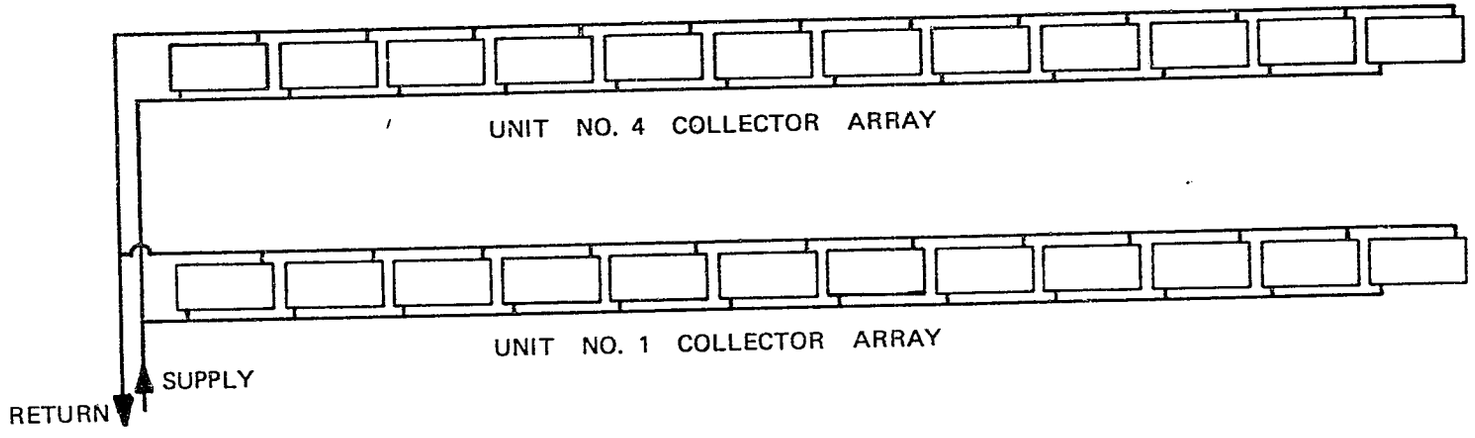

Collector Array Arangement

COLLECTOR ARRAY

TILT OF COLLECTORS – 65°
TILT OF SOLAR WINDOW – 30°
AZIMUTH – DUE SOUTH

SITE LOCATION

LATITUDE – 33°57′
LONGITUDE – 81°07′

Figure 3.2.1-1(b) Collector Details

The second viewpoint assumes that only the solar energy incident on the collector when the collector loop is operational be used in determining the collector array efficiency. The value of the operational incident solar energy used is multiplied by the ratio of the gross collector area to the gross collector array area to compensate for the difference between the two areas caused by installation spacing. The efficiency is then expressed by the equation:

$$\eta_{co} = Q_s/(Q_{oi} \times A_p/A_a) \qquad (2)$$

where η_{co} = Operational collector array efficiency

Q_s = Collected solar energy

Q_{oi} = Operational incident solar energy

A_p = Gross collector area (the product of the number of collectors and the envelope area of one collector)

A_a = Gross collector array area (total area including all mounting and connecting hardware and spacing of units)

The monthly efficiency computed by this method is listed in the column entitled "Operational Collector Array Efficiency" in Table 3.2.1-1.

In the ASHRAE Standard 93-77 a collector efficiency is defined in the same terminology as the operational collector array efficiency. However, the ASHRAE efficiency is determined from instantaneous evaluation under tightly controlled, steady state test conditions, while the operational collector array efficiency is determined from actual dynamic conditions of daily solar energy system operation in the field.

The ASHRAE Standard 93-77 definitions and methods often are adopted by collector manufacturers and independent testing laboratories in

TABLE 3.2.1-1

COLLECTOR ARRAY PERFORMANCE

Month	Incident Solar Energy (Million Btu)	Collected Solar Energy (Million Btu)	Collector Array Efficiency	Operational Incident Energy (Million Btu)	Operational Collector Array Efficiency
Jun 79	53.77	3.71	0.07	43.76	0.09
Jul 79	51.92	4.06	0.08	43.98	0.09
Aug 79	61.51	5.67	0.09	53.71	0.11
Sep 79	37.94	3.94	0.10	29.10	0.14
Oct 79	57.29	7.49	0.13	45.92	0.16
Nov 79	41.30	7.40	0.18	35.15	0.21
Dec 79	35.54	7.91	0.22	32.54	0.25
Jan 80	24.88	4.86	0.20	20.84	0.23
Feb 80	46.59	9.78	0.21	44.85	0.22
Mar 80	41.87	6.78	0.16	37.48	0.18
Apr 80	57.25	5.68	0.10	49.18	0.12
May 80	58.14	5.07	0.09	48.46	0.11
Total	568.00	72.35	--	484.97	--
Average	47.33	6.03	0.13	40.41	0.15

evaluating collectors. The collector evaluation performed for this report using the field data indicates that there was a significant difference between the estimated single panel collector data and the collector data determined from long term field measurements. This may or may not always be the case, and there are two primary reasons for differences when they exist:

- Test conditions are not the same as conditions in the field, nor do they represent the wide dynamic range of field operation (i.e. inlet and outlet temperature, flow rates and flow distribution of the heat transfer fluid, insolation levels, aspect angle, wind conditions, etc.).

- Collector tests are not generally conducted with units that have undergone the effects of aging (i.e. changes in the characteristics of the glazing material, collection of dust, soot, pollen or other foreign material on the glazing, deterioration of the absorber plate surface treatment, etc.).

Consequently field data collected over an extended period will generally provide an improved source of collector performance characteristics for use in long-term system performance definition.

The long-term data base for Wormser includes the months from March 1978 through May 1980. Although the solar energy system was in operation for most of the period, the solar system operated as designed only between June 1979 and May 1980. For consistency, the collector evaluation period was selected to be the same time interval.

The operational collector array efficiency data given in Table 3.2.1-1 are monthly averages based on instantaneous efficiency computations over the total performance period using all available data. For detailed collector analysis it was desirable to use a limited subset of the available data that characterized collector operation under "steady state" conditions. This subset was defined by applying the following restrictions:

(1) The measurement period was restricted to collector operation when the sun angle was within 30 degrees of the collector normal.

(2) Only measurements associated with positive energy gain from the collectors were used, i.e., outlet temperatures must have exceeded inlet temperatures.

(3) The sets of measured parameters were restricted to those where the rate of change of all parameters of interest during two regular data system intervals* was limited to a maximum of 5 percent.

Instantaneous efficiencies (η_j) computed from the "steady state" operation measurements of incident solar energy and collected solar energy by Equation (2)** were correlated with an operating point determined by the equation:

$$x_j = \frac{T_i - T_a}{I} \qquad (3)$$

where x_j = Collector operating point at the j^{th} instant

T_i = Collector inlet temperature

T_a = Outdoor ambient temperature

I = Rate of incident solar radiation

The data points (η_j, x_j) were then plotted on a graph of efficiency versus operating point and a first order curve described by the slope-intercept formula was fitted to the data through linear regression techniques. The form of this fitted efficiency curve is:

---

*The data system interval was 5-1/3 minutes in duration. Values of all measured parameters were continuously sampled at this rate throughout the performance period.

**The ratio A_p/A_a is assumed to be unity for this analysis.

$$\eta_j = b - mx_j \qquad (4)$$

where η_j = Collector efficiency corresponding to the j^{th} instant

b = Intercept on the efficiency axis

$(-)m$ = Slope

x_j = Collector operating point at j^{th} instant

The relationship between the empirically determined efficiency curve and the analytically developed curve will be established in subsequent paragraphs.

The analytically developed collector efficiency curve is based on the Hottell-Whillier-Bliss equation

$$\eta = F_R(\tau\alpha) - F_R U_L \left(\frac{T_i - T_a}{I}\right) \qquad (5)$$

where η = Collector efficiency

F_R = Collector heat removal factor

τ = Transmissivity of collector glazing

α = Absorptance of collector plate

U_L = Overall collector energy loss coefficient

T_i = Collector inlet fluid temperature

T_a = Outdoor ambient temperature

I = Rate of incident solar radiation

The correspondence between equations (4) and (5) can be readily seen. Therefore by determining the slope-intercept efficiency equation from measurement data, the collector performance parameters corresponding to the laboratory single panel data can be derived according to the following set of relationships:

$$b = F_R(\tau\alpha)$$
$$\text{and} \qquad (6)$$
$$m = F_R U_L$$

where the terms are as previously defined

The discussion of the collector array efficiency curves in subsequent paragraphs is based upon the relationships expressed in Equation (6). However, the single panel curve is not representative of the collector array performance expected of this system. This collector subsystem consists of 266 square feet of flat plate collectors (absorber plate area) augmented by pyramidal reflectors whose effective aperture varies from 295 square feet in July to 719 square feet in December (Figure 3.2.1-2 and 3.2.1-3). This is accomplished by a movable reflector (R1) shown in the figures. The tilt is proportional to the movement of the sun with respect to the local horizon. Without the movable reflector, no solar energy would be collected in the summer months. The purpose of the reflectors is to create a pseudo concentrating collector array whose concentration is highest during the winter months when the heating demands are greatest [12]. Figure 3.2.1-4 illustrates the effect of the concentration multiplier on the collector array performance. As the multiplier moves from 1 in summer to 2.9 in winter, the collector array efficiency increases from 0.08 to 0.247.

The collector array efficiencies indicated in Table 3.2.1-1 and Figure 3.2.1-4 are referenced to the solar window area which is 1152 square feet in conformance with National Bureau of Standards Performance Evaluation Procedures. However, collector analysis techniques usually utilize the collector absorber area as the reference area. The collector absorber area for the system is 266 square feet facing south at a tilt angle of 65°, located inside the attic of

JULY 18

AVERAGE DAILY SOLAR FOR JULY

SUN ANGLE = 27.01°

MOVABLE REFLECTOR TILT ANGLE = 40.23°

SUN TO HORIZON = 77.01°

EFFECTIVE AREA = 294.55 FT^2

COLLECTOR AREA = 266.33 FT^2

MULTIPLIER = $\frac{294.55}{266.33}$ = 1.11

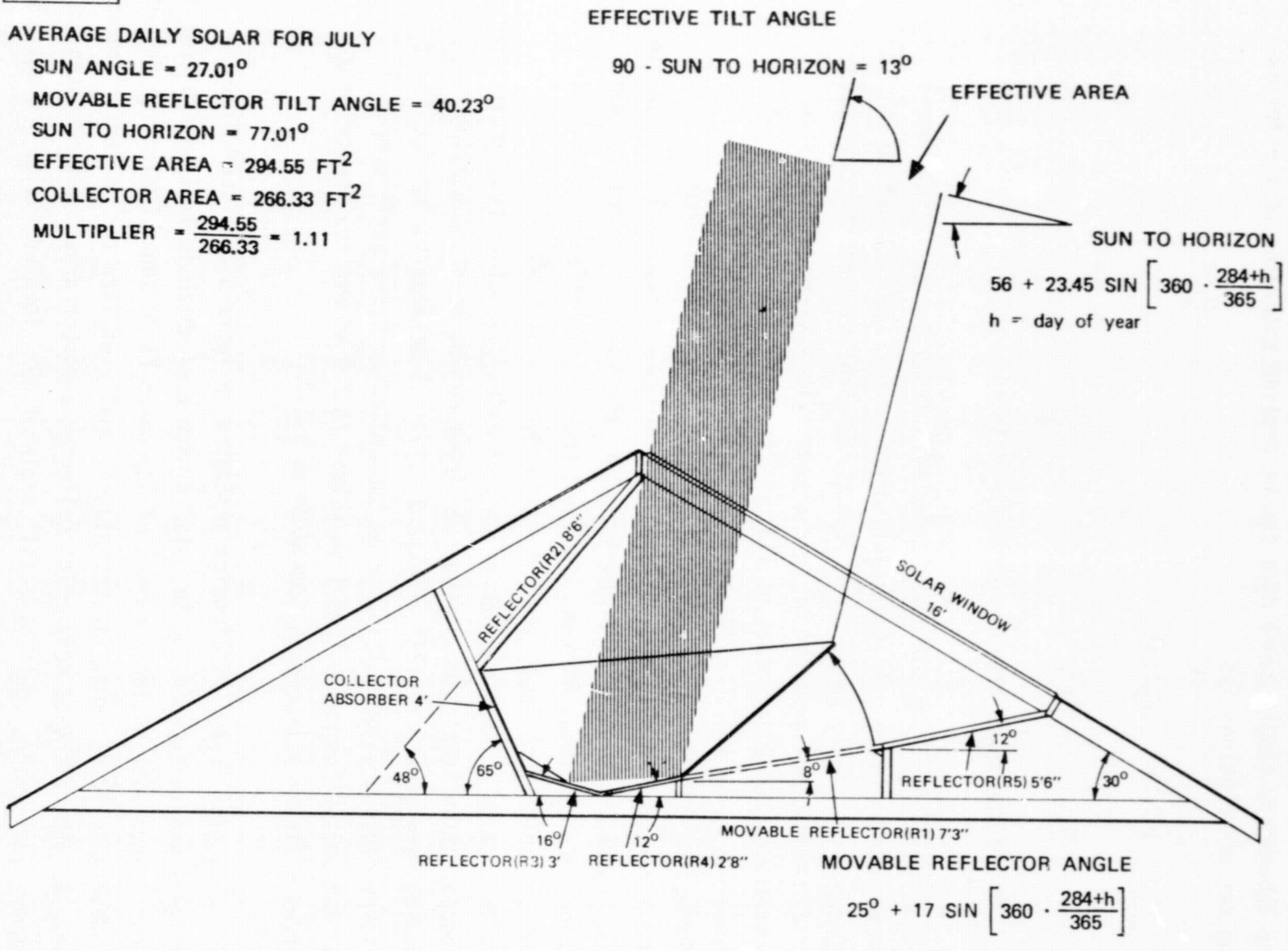

Figure 3.2.1-2 Wormser Pyramidal Optical Cavity for July

DECEMBER 10

AVERAGE DAILY SOLAR FOR DECEMBER

SUN ANGLE = -23.05^{o}

MOVABLE REFLECTOR TILT ANGLE = 8.29^{o}

SUN TO HORIZON = 32.95^{o}

EFFECTIVE AREA = 719.3 FT^2

COLLECTOR AREA = 266.33 FT^2

MULTIPLIER = $\frac{719.3}{266.33} = 2.67$

SUN TO HORIZON ANGLE

$56 + 23.45 \text{ SIN } \left[360 \cdot \frac{284+h}{365}\right]$

h = day of year

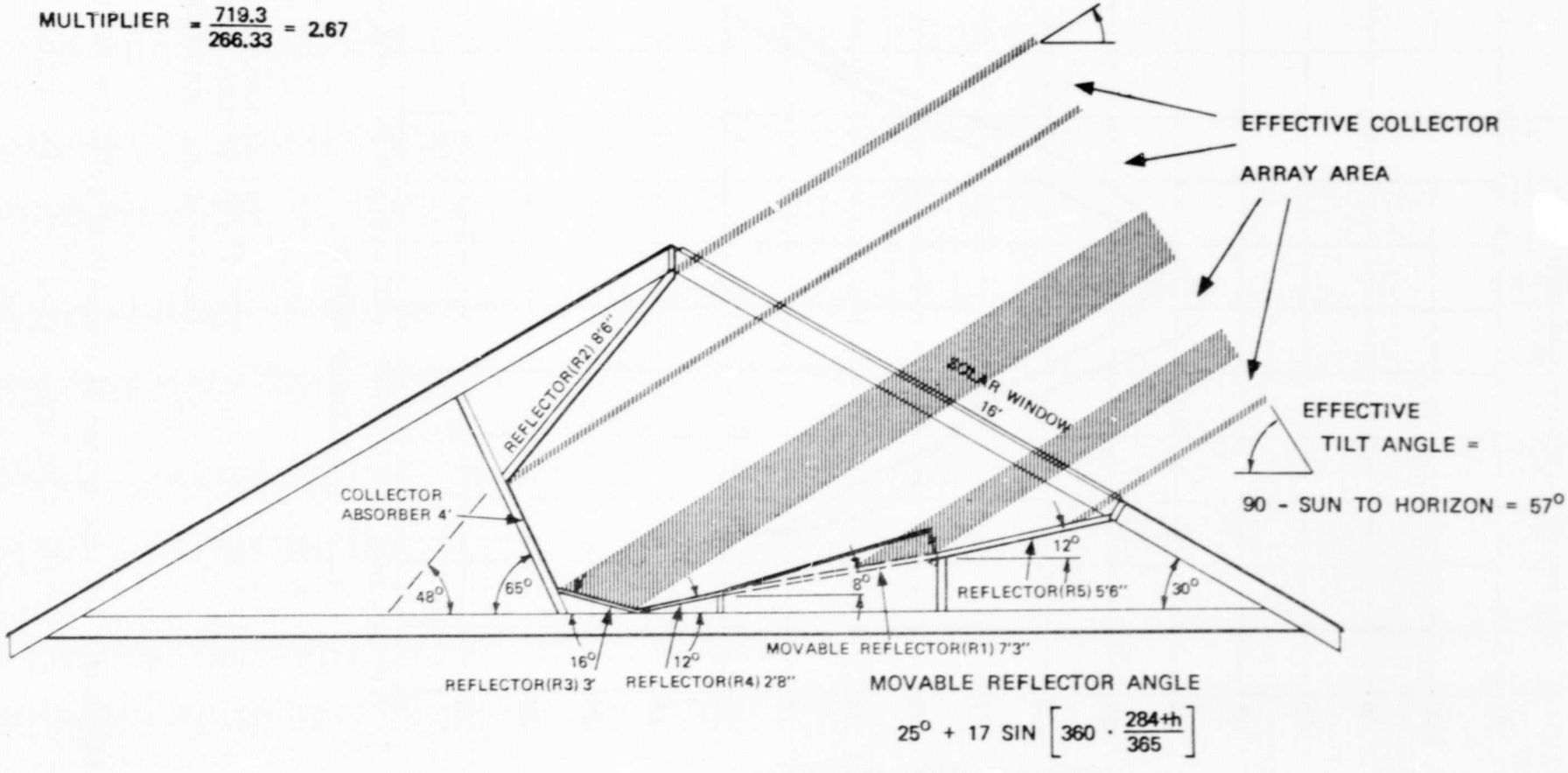

MOVABLE REFLECTOR ANGLE

$25^{o} + 17 \text{ SIN } \left[360 \cdot \frac{284+h}{365}\right]$

Figure 3.2.1-3 Wormser Pyramidal Optical Cavity for December

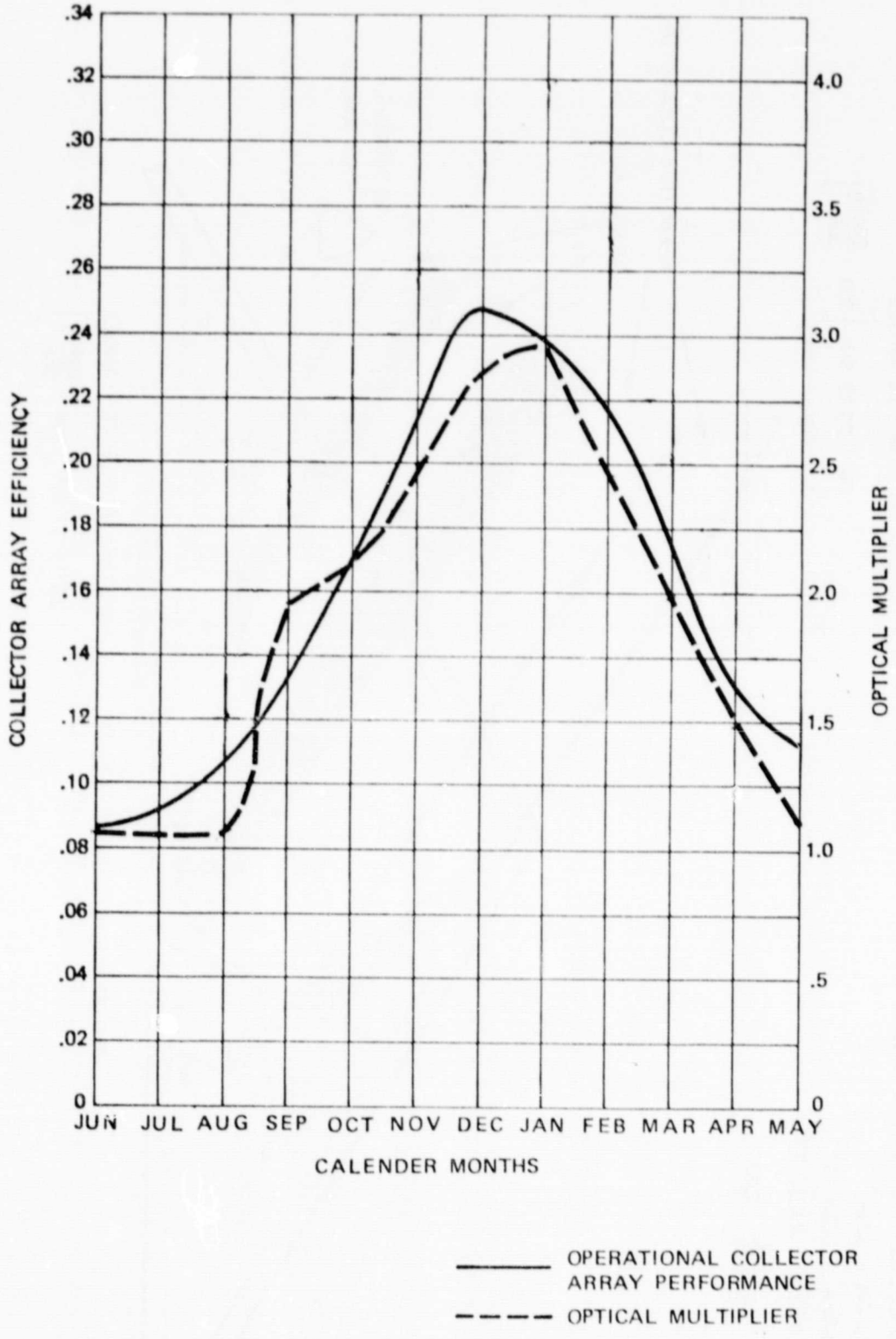

Figure 3.2.1-4 Comparison of Operational Collector Vs. Pyramidal Multiplier

two of the townhouses. Figure 3.2.1-5 shows the collector array efficiency, referenced to both the absorber area and the solar window area. Plotted in the figure is the actual performance and the actual performance divided by the concentration multiplier for both reference areas. The collector performance curve that most accurately portrays how this collector array performs is the curve showing actual performance divided by the multiplier and reference to the absorber area. This curve indicates that the collector array efficiency lies somewhere between .3 and .4 for the 12 month evaluation period. This result indicates that the array is performing quite similar to an array of flat plate collectors. Thus all subsequent paragraphs discuss the collector array efficiency referenced to the absorber area with the multiplier effect removed. In order to utilize the field derived collector analysis program [10], the multiplier (effective area) had to be removed and an effective tilt determined. Figures 3.2.1-2 and 3.2.1-3 illustrate how the effective tilt and effective area are derived for the months July and December. The same technique is utilized for all other months to obtain these same parameters.

In deriving the collector array efficiency curves by the linear regression technique, measurement data over the entire performance period yields higher confidence in the results than similar analysis over shorter periods. Over the longer periods the collector array is forced to operate over a wider dynamic range. This eliminates the tendency shown by some types of solar energy systems* to cluster efficiency values over a narrow range of operating points. The clustering effect tends to make the linear regression technique approach constructing a line through a single data point. The use of data from the entire performance period results in a collector array efficiency curve that is more accurate in long-term solar system performance prediction. The long-term curves for July and December and the estimated performance curve derived from the laboratory single panel data are shown in Figure 3.2.1-6. The estimated performance curve was obtained by using single panel performance data [3] from another site (Colt Yosemite) that

* Single tank hot water systems show a marked tendency toward clustering because the collector inlet temperature remains relatively constant and the range of values of ambient temperature and incident solar energy during collector operation are also relatively restricted on a short term basis.

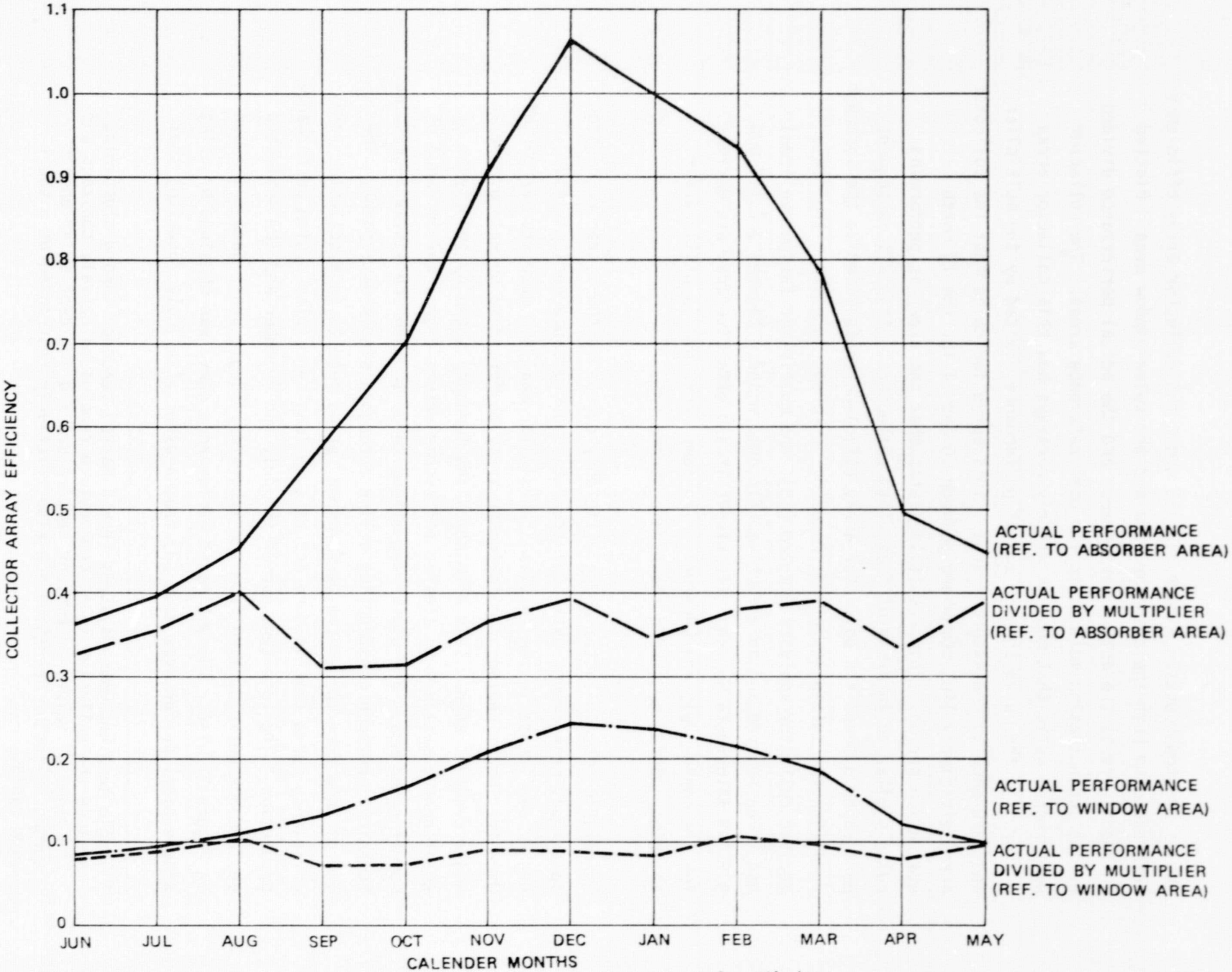

Figure 3.2.1-5 Collector Efficiency Referenced to Both the Solar Window and Collector Absorber Area Vs. Calendar Months

utilized the same absorber in the collector array and modifying that data to account for differences in transmissivity properties of the Plexiglas glazing and the increased insulation (6 inches instead of 3 inches of fiberglass) associated with this array. As can be seen, the estimated performance curve lies between the July and December performance curves which represent the bounds in performance variations of the collector array. The estimated curve is closest to the December curve for low operating points and closest to the July curve for high operating points. The lower slope associated with the December operating curve can be attributed to lower array loss that occurs when the array is essentially collecting solar beam radiation reinforced by the pyramided reflectors. The higher slope associated with the July operating curve is due to reflecting losses associated with the movable reflector which is necessary to obtain any solar energy during summer months.

For information purposes the data associated with Figure 3.2.1-2 is as follows:

Estimated single panel laboratory data

$F_R(\tau\alpha) = 0.509$ $\quad\quad$ $F_R U_L = -0.65$

Long-term field data (July)

$F_R(\tau\alpha) = 0.396$ $\quad\quad$ $F_R U_L = -0.536$

Long-term field data (December)

$F_R(\tau\alpha) = 0.468$ $\quad\quad$ $F_R U_L = -0.266$

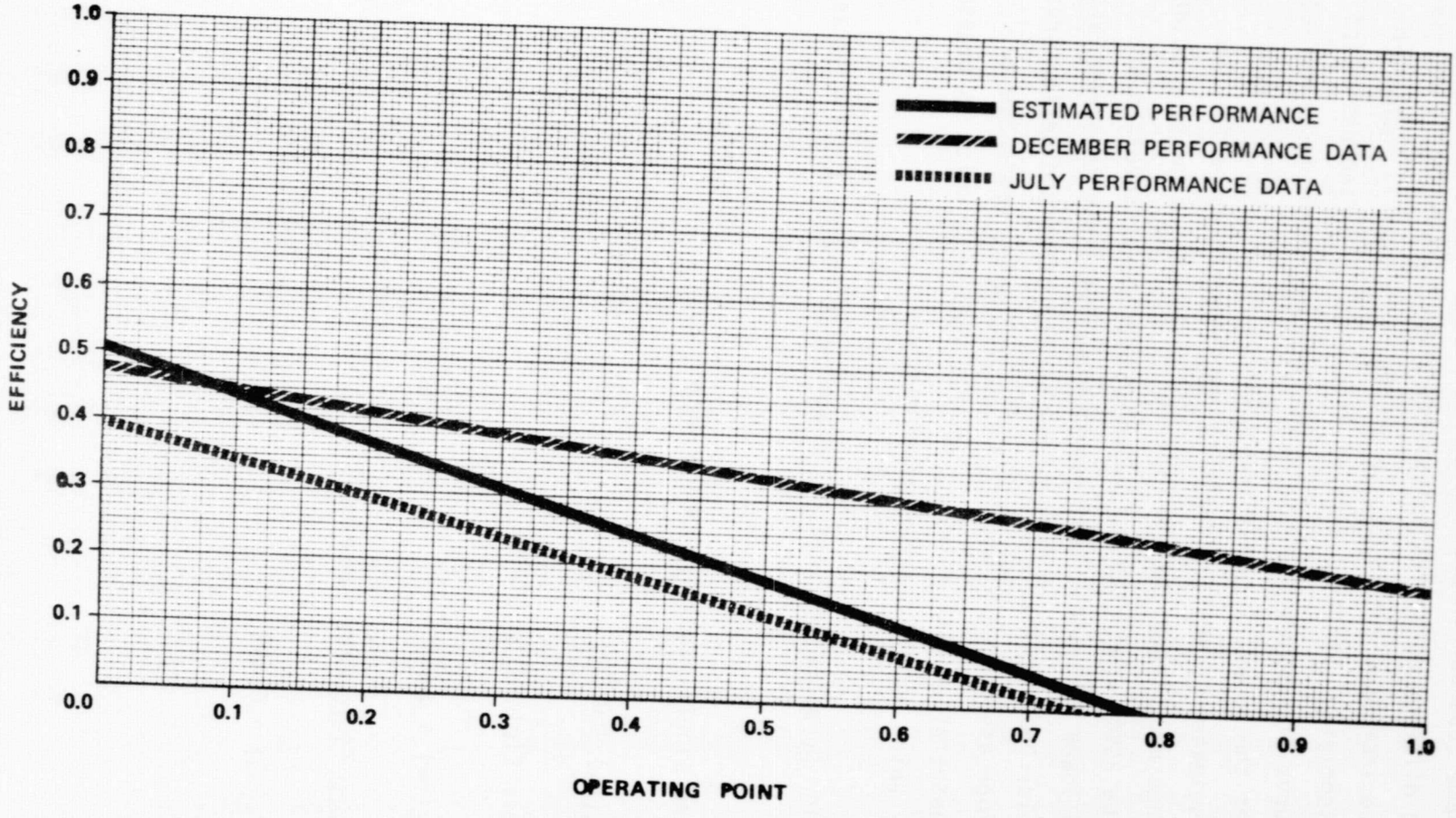

Figure 3.2.1-6 Wormser Collector Efficiency Curves

A histogram of collector array operating points illustrates the distribution of instantaneous values as determined by Equation (3) for the entire month. The histogram was constructed by computing the instantaneous operating point value from site instrumentation measurements at the regular data system intervals throughout the month, and counting the number of values within contiguous intervals of width 0.01 from zero to unity. The operating point histogram shows the dynamic range of collector operation during the month from which the midpoint can be ascertained. The average collector array efficiency for the month can then be derived by projecting the midpoint value to the appropriate efficiency curve and reading the corresponding value of efficiency.

Another characteristic of the operating point histogram is the shifting of the distribution along the operating point axis. This can be explained in terms of the characteristics of the system and the climatic factors of the site, i.e., incident solar energy and ambient temperature. Figure 3.2.1-7 shows two histograms that illustrate a typical winter month (December) and a typical summer month (July) operation. The approximate average operating point for December is at 0.12 and for July at 0.09. The operating point for this array moves very little throughout the 12 month evaluation period. The reason is the design of the collectors and the relatively small change in storage temperature.

Also shown in Figure 3.2.1-7 on the December operating point histogram is the monthly collector array efficiency of 0.39 for December (Figure 3.2.1-5) and the December field derived collector array efficiency curve. The intersection of the average operating point for December and the December performance curve implied a monthly efficiency of 0.41. The close agreement between the field derived collector array efficiency and the actual December monthly collector performance indicates that the field derived performance data could be used for design purposes.

Additional information concerning collector array analysis in general may be found in Reference [10]. The material in the reference describes the detailed collector array analysis procedure and presents the results of analyses performed on numerous collector array installations across the United States.

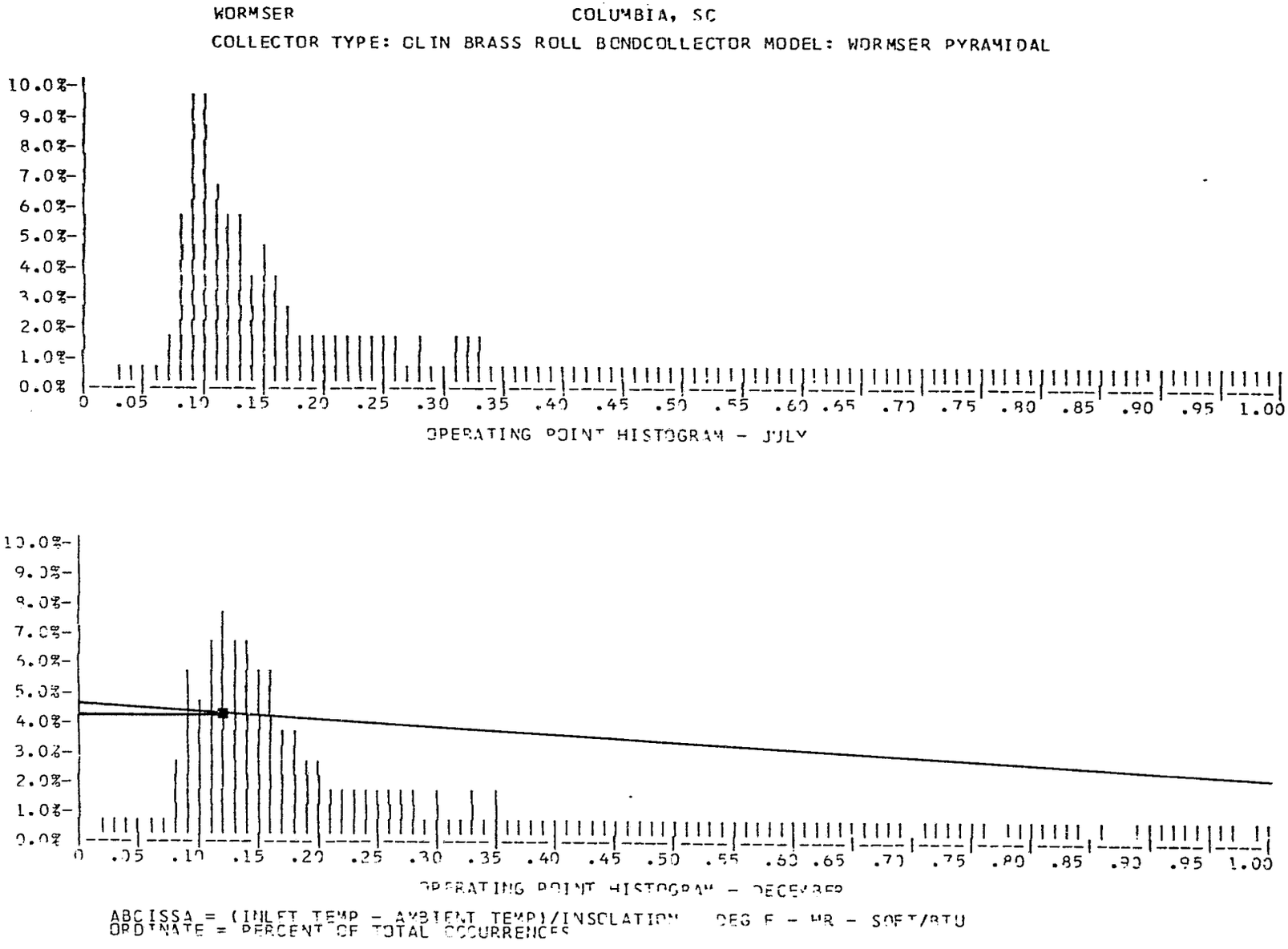

Figure 3.2.1-7 Wormser Operating Point Histograms for Typical Winter and Summer Months

3.2.2 Storage Subsystem

Storage subsystem performance is described by comparison of energy to storage, energy from storage and change in stored energy. The ratio of the sum of energy from storage and change in stored energy to energy to storage is defined as storage efficiency, η_s. This relationship is expressed in the equation

$$\eta_s = (\Delta Q + Q_{so})/Q_{si} \quad (7)$$

where:

ΔQ = Change in stored energy. This is the difference in the estimated stored energy during the specified reporting period, as indicated by the relative temperature of the storage medium (either positive or negative value)

Q_{so} = Energy from storage. This is the amount of energy extracted by the load subsystem from the primary storage medium

Q_{si} = Energy to storage. This is the amount of energy (both solar and auxiliary) delivered to the primary storage medium

Evaluation of the system storage performance under actual system operation and weather conditions can be performed using the parameters defined above. The utility of these measured data in evaluation of the overall storage design can be illustrated in the following discussion.

Table 3.2.2-1 summarizes the storage subsystem performance during the report period. During the twelve month period, a total of 69.42 million Btu was delivered to the storage tanks and a total of 46.98 million Btu was removed for support of system loads. The net change in stored energy during this same time period was 0.26 million Btu, which leads to a storage efficiency of 0.68 and a total energy loss from storage of 22.18 million Btu.

The computed storage efficiency of 0.68 is relatively low as compared to most solar energy systems. The average storage temperature during the period that efficiency was computed was only 101°F, so a high value of efficiency is expected. Thus, there must be significant solar storage tank losses present. The storage subsystem losses occur when the energy is being transported to meet the space heating demand. The transport piping is insulated but the run lengths are long which results in large losses. However, this is not meant to detract in any way from the fact that the storage subsystem performed well during the reporting period. The system is well insulated and the effective heat transfer coefficient averaged 95.5 Btu/Hr-°F during the period.

An effective storage heat transfer coefficient for the storage subsystem can be defined as follows:

$$C = (Q_{si} - Q_{so} - \Delta Q)/[\bar{T}_s - \bar{T}_a) \times t] \frac{Btu}{Hr-°F} \qquad (8)$$

where

C = Effective storage heat transfer coefficient

TABLE 3.2.2-1

STORAGE SUBSYSTEM PERFORMANCE

Month	Energy To Storage (Million Btu)	Energy From Storage (Million Btu)	Change In Stored Energy (Million Btu)	Storage Efficiency	Storage Average Temperature (°F)	Basement Temperature (°F)	Effective Storage Heat Loss Coefficient (Btu/Hr°F)
Jun 79	3.71	1.80	0.11	0.52	112	75	67.5
Jul 79	4.06	2.19	0.10	0.57	114	76	62.6
Aug 79	5.67	3.35	0.15	0.62	119	76	67.8
Sep 79	3.94	2.13	-0.32	0.46	117	74	68.8
Oct 79	7.46	3.42	0.38	0.51	130	70	82.0
Nov 79	7.11	5.03	-0.80	0.60	107	68	102.6
Dec 79	7.46	5.82	-0.21	0.75	85	66	130.9
Jan 80	4.71	3.69	0.05	0.79	78	62	81.5
Feb 80	8.41	6.83	0.24	0.84	69	60	213.9
Mar 80	6.23	5.45	-0.21	0.84	72	63	147.9
Apr 80	5.59	3.64	0.63	0.77	96	70	70.5
May 80	5.07	3.63	0.14	0.74	109	74	49.9
Total	69.42	46.98	0.26	--	--	--	--
Average	5.79	3.92	0.02	0.68	101	70	95.5

Q_{si} = Energy to storage

Q_{so} = Energy from storage

ΔQ = Change in stored energy

$\overline{T}_s$ = Storage average temperature

$\overline{T}_a$ = Average ambient tempeature in the vicinity of storage

t = Number of hours in the month

The effective storage heat transfer coefficient is comparable to the heat loss rate defined in ASHRAE Standard 94-77 [9]. It has been calculated for each month in this report period and included, along with an assumed basement average temperature, in Table 3.2.2-1.

Examination of the values for the effective storage heat transfer coefficient shows that the variation is quite significant. The storage heat loss is highest during the coldest winter months and lowest during the spring and fall. Overall, the heat loss coefficient is low which is indicative of a properly performing liquid storage system.

3.2.3 Hot Water Subsystem

The performance of the hot water subsystem is described by comparing the amount of solar energy supplied to the subsystem with the energy required to satisfy the total hot water load. The energy required to satisfy the total load consists of both solar energy and auxiliary thermal energy.

The performance of the Wormser hot water subsystem is presented in Table 3.2.3-1. The value for auxiliary energy supplied in Table 3.2.3-1 is the gross energy supplied to the auxiliary system. The value of auxiliary energy supplied multiplied by the auxiliary system efficiency gives the auxiliary thermal energy actually delivered to the load. The difference between the sum of auxiliary thermal energy plus solar energy and the hot water load is equal to the thermal (standby) losses from the hot water subsystem.

The measured solar fraction in Table 3.2.3-1 is an average weighted value for the month based on the ratio of solar energy in the hot water tank to the total energy in the hot water tank when a demand for hot water exists. This value is dependent on the daily profile of hot water usage. It does not represent the ratio of solar energy supplied to the sum of solar plus auxiliary energy supplied shown in the Table.

For the 12 month period from April 1979 through May 1980, the solar energy system supplied a total of 22.46 million Btu to the hot water load. The total hot water load for this period was 62.88 million Btu, and the weighted average monthly solar fraction was 23 percent.

The monthly average hot water load during the reporting period was 5.24 million Btu. This is based on an average daily consumption of 254 gallons, delivered at an average temperature of 151°F and supplied to the system at an average temperature of 71°F. The temperature of the supply water ranged from a low of 62°F in February to a high of 79°F in September.

Each month an average of 1.87 million Btu of solar energy and 5.19 million Btu of auxiliary thermal (electrical) energy were supplied to the hot water subsystem. Since the average monthly hot water load was 5.24 million Btu, an average of 1.82 million Btu was lost from the hot water tank each month. These high losses are attributable to the high hot water demand and large energy transport losses associated with long piping run lengths.

Table 3.2.3-1

HOT WATER SUBSYSTEM PERFORMANCE

Month	Hot Water Parameters				Energy Consumed (Million Btu)			Weighted Solar Fraction (Percent)
	Load (Million Btu)	Gallons Used	Temperatures (°F) Supply	Delivery	Solar	Auxiliary Thermal	Auxiliary	
Jun 79	1.18	2,064	73	142	1.78	1.47	1.47	52
Jul 79	3.49	5,820	75	149	2.19	3.40	3.40	38
Aug 79	3.96	7,162	78	149	3.35	3.29	3.29	49
Sep 79	4.42	7,654	79	154	2.12	4.00	4.00	33
Oct 79	5.51	9,115	75	149	2.69	4.77	4.77	35
Nov 79	5.79	9,298	71	149	1.27	5.51	5.51	17
Dec 79	6.84	9,514	66	152	0.49	6.01	6.01	7
Jan 80	7.03	9,125	63	154	1.33	6.68	6.68	16
Feb 80	6.53	8,254	62	154	0.63	9.03	9.03	5
Mar 80	6.53	8,442	63	154	0.77	7.24	7.24	10
Apr 80	5.92	7,966	68	154	2.39	6.05	6.05	27
May 80	5.68	8,331	73	155	3.51	4.83	4.83	41
Total	62.88	92,745	--	--	22.46	62.28	62.28	--
Average	5.24	7,729	71	151	1.87	5.19	5.19	23 **

** Weighted solar fraction = $$\frac{\sum_{1}^{12} HWSFR_i \times HWL_i}{HWL}$$

where HWL = Hot Water Load
HWSFR = Hot Water Solar Fraction

3.2.4 Space Heating Subsystem

The performance of the space heating subsystem is described by comparing the amount of solar energy supplied to the subsystem with the energy required to satisfy the total space heating load. The energy required to satisfy the total load consists of both solar energy and auxiliary thermal energy. The ratio of solar energy supplied to the load to the total load is defined as the heating solar fraction. The calculated heating solar fraction is the indicator of performance for the subsystem because it defines the percentage of the total space heating load supported by solar energy.

The performance of the Wormser space heating subsystem is presented in Table 3.2.4-1. For the 12 month period from April 1979 through May 1980, the solar energy system supplied a total of 27.45 million Btu to the space heating load. The total heating load for this period was 65.04 million Btu, and the average monthly solar fraction was fourty-two percent.

It must be emphasized that all values presented in this section relating to the performance of the space heating subsystem are based on measured parameters. In other words the space heating load, solar contribution and auxiliary thermal energy used are all determined based on the measured output of the space heating subsystem. These measured values do not include any of the various solar energy losses that are present in the system. However, solar energy losses are generally added to the interior of the building and, as such, represent an uncontrolled (unmeasured) contribution to the space heating load. At the Wormser site these solar energy losses occur during energy transport between the various subsystems and, to a lesser extent, from the storage tank and the domestic hot water tank. Thus, uncontrolled energy contribution can occur. These energy contributions may have contributed to meeting the space heating demand.

TABLE 3.2.4-1

HEATING SUBSYSTEM PERFORMANCE

Month	Heating Parameters			Solar	Energy Consumed (Million Btu)		Measured Solar Fraction (Percent)
	Load (Million Btu)	Temperatures (°F)			Auxiliary Thermal	Auxiliary	
		Building	Outdoor				
Jun 79	0.00	75	75	0.00	0.00	0.00	0
Jul 79	0.00	75	78	0.00	0.00	0.00	0
Aug 79	0.00	74	80	0.00	0.00	0.00	0
Sep 79	0.32	74	73	0.01	0.31	0.32	3
Oct 79	0.93	73	64	0.76	0.04	0.05	82
Nov 79	4.57	72	57	4.06	0.42	0.49	89
Dec 79	13.22	71	48	5.78	3.67	4.51	44
Jan 80	15.44	70	44	2.51	6.62	7.71	16
Feb 80	17.40	70	43	7.57	9.61	11.15	44
Mar 80	11.42	71	51	5.23	6.14	7.15	46
Apr 80	1.59	73	64	1.41	0.19	0.20	89
May 80	0.15	75	71	0.12	0.01	0.01	82
Total	65.04	--	--	27.45	27.01	31.59	--
Average	5.42	73	62	2.29	2.25	2.63	42 *

* Measured average solar fraction is weighted by load.

During the reporting period (April 1979 through May 1980) a total of approximately 22.44 million Btu of solar energy was added to the space heating load through these various losses. The loss occurred mainly from the storage tank (22.18 million Btu). This amount of uncontrolled solar energy is fourty-five percent of the total solar energy delivered to meet the heating demands. Now if these losses are considered to have met the space heating demand, then the total solar delivered to the space heating demand would have been 49.89 million Btu, the solar fraction fifty-seven percent and the total space heating demand 87.48 million Btu. Thus, the performance of the space heating subsystem would be substantially increased.

Figure 3.2.4-1 illustrates the auxiliary heat pump performance and indicated load variations for each of the townhouse apartments. The results indicate that the heat pumps operating in the air-to-air mode are performing as expected because of the close agreement between the actual heating capacity and power inputs and the manufacturers predicted performance curves [5]. Also indicated in the figures are the occupied and unoccupied building heat loss coefficients (UA). The heat loss coefficient for Apartment No. 1 when occupied is substantially lower than that of the other apartments. The lower UA for Apartment No. 1 is due to the substantial solar energy losses occurring from the solar storage tank which is located in the basement of Apartment No. 1.

Figure 3.2.4-2 illustrates the performance of the heat pumps operating in the heat pump solar mode 3. The performance of the heat pumps for units 1 and 4 is quite low during winter months and near that expected in fall and spring. Also heat pumps for units 2 and 3 are lower than normal in winter and higher than normal in spring and fall. The reason for these circumstances is not known but this condition has a substantial effect on the indicated space heating demand when operating in this mode. The power input is near that expected but the indicated heat pump performance capacities are below normal.

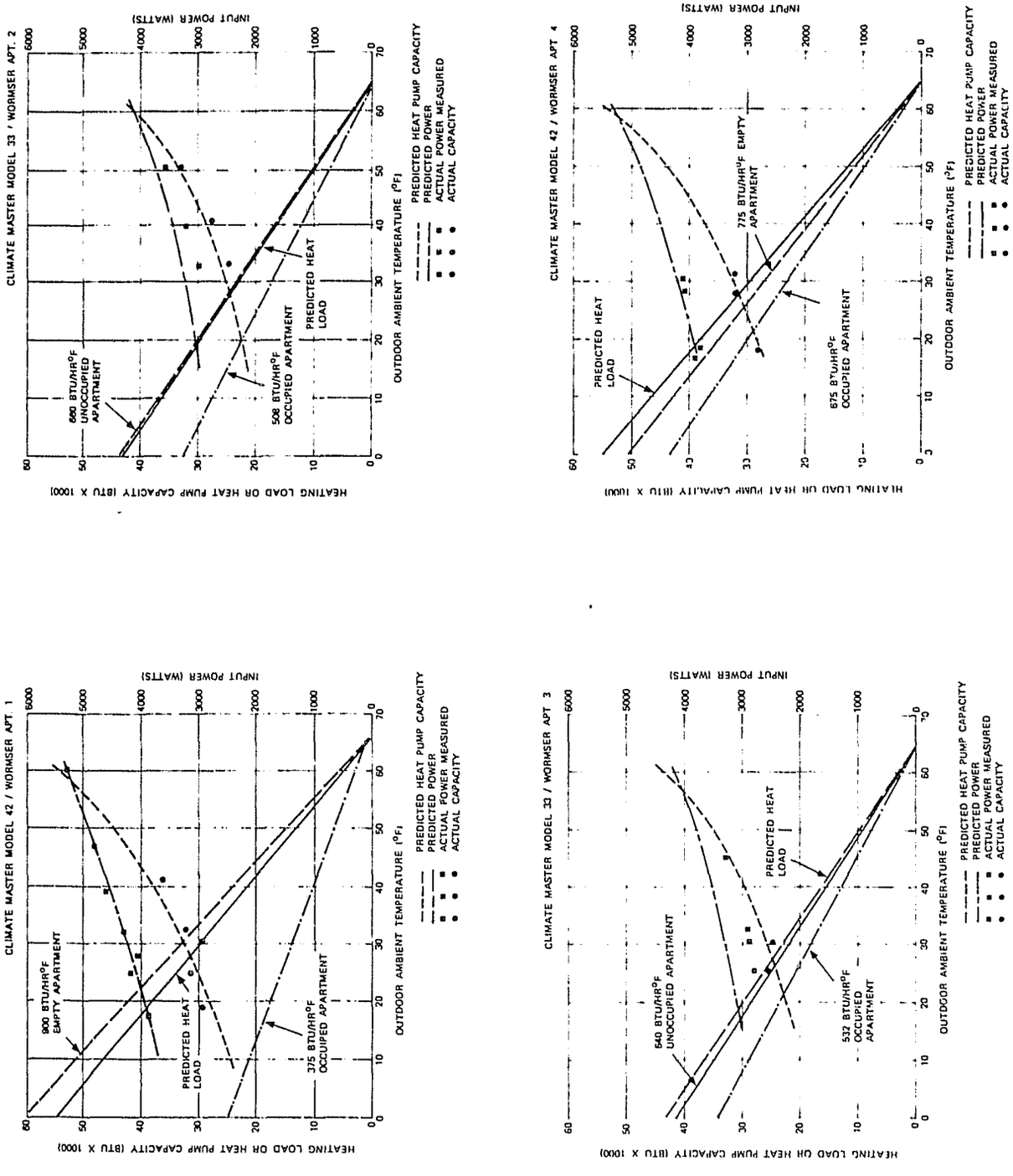

Figure 3.2.4-1 Wormser Auxiliary Heat Pump Performance Vs. Indicated Heating Loads

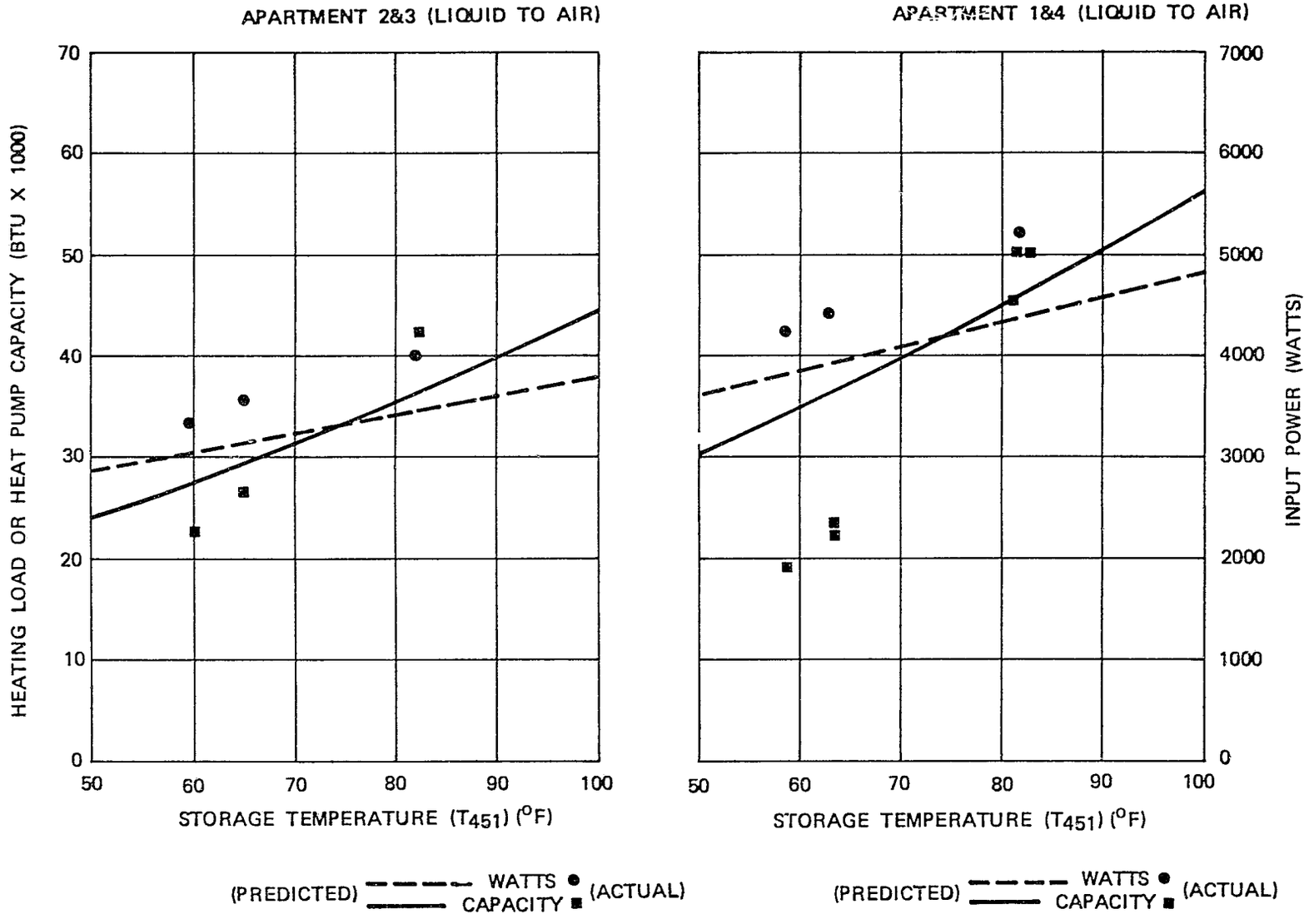

Figure 3.2.4-2 Wormser Heat Pump/Solar Performance

The performance of the solar system operating in the direct solar mode was found to be close to that expected. However, because of control problems, this mode was not exercised as much as desired.

The effect of the system operating modes on the performance of the space heating subsystem is illustrated in Table 3.2.4-2. The coefficient of performance of the entire system is lowest in the winter months when the undesirable solar plus heat strip mode was occurring. If the problem could have been eliminated, the system performance would have been greater. This can be illustrated by comparing December 1979 with March 1980 whose heating demands are nearly the same. The solar plus heat strip mode was exercised less in December and as such the coefficient of performance was 2.63 as compared to 1.42 for March. The coefficient of performance for the spring and fall months was very high which is indication of the effect of the solar only mode performance.

During the 12 month reporting period a total of 31.59 million Btu of auxiliary energy was consumed by the space heating subsystem in order to supply 27.01 million Btu of thermal energy to supplement solar energy. Approximately 9255 Kwh of electricity were needed to support the space heating subsystem.

TABLE 3.2.4-2

THERMAL CONVERSION EQUIPMENT PERFORMANCE

Month	Equipment Load (Million Btu)	Thermal Energy Input (Million Btu)	Coefficient Of Performance
Jun 79	0	0	0
Jul 79	0	0	0
Aug 79	0	0	0
Sep 79	0.32	0.32	1.00
Oct 79	0.93	0.07	13.40
Nov 79	4.57	0.81	5.67
Dec 79	13.22	5.03	2.63
Jan 80	15.44	7.97	1.94
Feb 80	17.40	12.48	1.39
Mar 80	11.42	8.02	1.42
Apr 80	1.59	0.35	4.56
May 80	0.15	0.01	11.34
Total	65.04	35.06	----
Average	5.42	2.92	1.86

4. OPERATING ENERGY

Operating energy for the Wormser Solar Energy System is defined as the energy required to transport solar energy to the point of use. Total operating energy for this system consists of energy collection and storage subsystem operating energy, hot water subsystem operating energy and space heating subsystem operating energy. Operating energy is electrical energy that is used to support the subsystems without affecting their thermal state. Measured monthly values for subsystem operating energy are presented in Table 4-1.

Total system operating energy for the Wormser Solar Energy System is that electrical energy required to operate the pumps in the energy transport subsystem and the air circulating fan. These are shown as EP101, EP301, EP405 and portions of EP401 through EP404, respectively, in Figure 2-1. Although additional electrical energy is required to operate the valves in the energy transport subsystem and the control system for the installation, it is not included in this report. These devices are not monitored for power consumption and the power they consume is inconsequential when compared to the pump motor powers and fan motor power.

During the 12 month reporting period, a total of 29.67 million Btu (8693 kWh) of operating energy was consumed. However, this includes the energy required to operate the blower in the supply duct, and that energy would be required whether or not the solar energy system was being utilized for space heating. Therefore, the energy consumed by the circulating fan is not considered to be solar peculiar operating energy, even though it is included as part of the the space heating subsystem operating energy.

A total of 14.98 million Btu (4389 kWh) of operating energy was required to support the pumps that are unique to the solar energy system during the reporting period. Of this total, 7.25 million Btu were allocated to the Energy Collection and Storage Subsystem (ECSS), 3.49 million Btu were allocated to the solar portion of the space heating subsystem, and 4.24 million Btu were allocated to the hot water subsystem. A total of 14.98 million Btu were allocated to space heating circulating fan. This additional energy is included in the total system operating energy. Since a measured 49.91 million Btu of solar energy was delivered to system loads during the reporting reporting period, a total of 0.30 million Btu (88 kWh) of operating energy was was required for each one million Btu of solar energy delivered to the system loads.

TABLE 4-1

OPERATING ENERGY

Month	Solar ECSS Operating Energy (Million Btu)	Space Heating Solar Operating Energy (Million Btu)	Hot water Heating Solar Operating Energy (Million Btu)	Total System Solar Operating Energy (Million Btu)	Space Heating Circulating Fan Energy (Million Btu)	Total Operating Energy Energy (Million Btu)
Jun 79	0.68	0.00	0.23	0.91	0.00	0.91
Jul 79	0.73	0.00	0.32	1.05	0.00	1.05
Aug 79	0.76	0.00	0.45	1.21	0.00	1.21
Sep 79	0.41	0.00	0.32	0.73	0.00	0.73
Oct 79	0.48	0.02	0.35	0.85	2.11	2.96
Nov 79	0.46	0.32	0.29	1.07	1.71	2.78
Dec 79	0.50	0.52	0.38	1.40	1.64	3.04
Jan 80	0.34	0.26	0.50	1.10	2.43	3.53
Feb 80	0.81	1.35	0.41	2.57	2.45	5.02
Mar 80	0.82	0.87	0.20	1.89	1.98	3.87
Apr 80	0.62	0.15	0.34	1.11	2.37	3.48
May 80	0.64	0.00	0.45	1.09	0.00	1.09
Total	7.25	3.49	4.24	14.98	14.69	29.67
Average	0.60	0.29	0.35	1.25	1.22	2.47

5. ENERGY SAVINGS

Solar energy system savings are realized whenever energy provided by the solar energy system is used to meet system demands which would otherwise be met by auxiliary energy sources. The operating energy required to provide solar energy to the load subsystems is subtracted from the solar energy contribution, and the resulting energy savings are adjusted to reflect the coefficient of performance (COP) of the auxiliary source being supplanted by solar energy.

The Wormser Solar Energy System utilizes multimode heat pumps for auxiliary electrical space heating and auxiliary energy for water heating is provided by electric elements in the DHW tanks. The electrical hot water heating element is considered to be 100 percent efficient. Energy savings for the 12 month reporting period are presented in Table 5-1. During this time the system realized a gross electrical energy savings of 19.34 million Btu. However, a total of 14.98 million Btu of electrical operating energy was required to support the solar energy system, so the net electrical energy savings was 4.36 million Btu, or 1277 kWh. If the undesirable solar plus heat mode had been eliminated, the total savings would have been 14.72 million Btu or 4313 kWh. This is equivalent to 2.5 barrels of oil. The net electrical savings associated with this system is quite low in view of the substantial solar energy contributions indicated in the space heating and hot water subsystem reports. The low indicated electrical savings is due to control problems associated with the heat pump solar mode 3. The solar system operated entirely too often in the solar plus heat strip mode. This mode is inefficient because a substantial amount of energy is being consumed at a COP of unity. Normally the COP in the heat pump solar mode 3 would be on the order of 2 to 2.5. Thus, during the winter months, the system performance was degraded. If the solar plus heat strip mode had been eliminated then 12.89 million Btu of additional energy could have been saved (Table 5-1). The electrical saving would then have been 22.35 million Btu for the hot water subsystem and 17.25 million Btu for the space heating subsystem for a total of 30.60 million Btu. This figure

is close to the indicated solar contribution of 49.91 million Btu. However, after the operating energy costs are accounted for the total savings accrued would have been 23.62 million Btu or 7214 kWh. This amount of savings is significantly higher than the actual savings but still low for a system collecting as much energy as this system did.

It should be noted that all values relating to space heating savings are based only on the measured solar energy contribution to the space heating load. As discussed in the space heating subsystem section, approximately 22.44 million Btu of solar energy were added to the interior of Townhouse Apartment No. 1 during the heating season. This uncontrolled addition of solar energy to the Townhouse represents an additional savings of approximately 9.63 million Btu;

$$\frac{\text{Solar Loss Contributions}}{\text{HP (Air-To-Air) COP}} = \frac{22.44}{2.33} = 9.63$$

The previous savings indications illustrate how difficult it is for a solar system to compete with a heat pump auxiliary subsystem. The space heating savings accrued are substantially lower than the solar energy contribution to the subsystem. Operating the system in the direct solar mode would have achieved greater savings and should be considered as an alternate to the multimode heat pump operation. The space heating system net savings would have been increased to (27.45 - 3.49) or 23.96 million Btu if the solar only mode would have been utilized exclusively. Another alternate would be to utilize the space heating subsystem solar energy to heat hot water. The solar system savings would have been much greater. The 27.45 million Btu which supported the space heating load would have resulted in a net savings of 23.21 million Btu;

$$\text{Solar Energy Delivered} - \text{Operating Energy Projection}$$
$$= 27.45 - 4.24 = 23.21$$

TABLE 5-1

ENERGY SAVINGS

Month	Electrical Energy Savings (Million Btu) Hot Water	Electrical Energy Savings (Million Btu) Space Heating	Solar Operating Energy (Million Btu)	Net Savings			Total Savings* Fossil Equivalent At Source (Million Btu)	Total Savings Fossil Equivalent At Source After Elimination of Solar Plus Heat Strip Mode*** (Million Btu)
				Electrical		Elimination of Solar Plus Heat Strip Mode**		
				Million Btu	kWh			
Jun 79	1.78	0.00	0.91	0.87	255	0.00	2.89	2.89
Jul 79	2.19	0.00	1.05	1.14	334	0.00	3.78	3.78
Aug 79	3.35	0.00	1.21	2.14	627	0.00	7.12	7.12
Sep 79	2.12	-0.18	0.73	1.21	355	0.00	4.03	4.03
Oct 79	2.69	0.31	0.85	2.15	630	0.00	7.17	7.17
Nov 79	1.27	1.35	1.07	1.55	454	0.20	5.17	5.83
Dec 79	0.49	0.86	1.40	-0.05	-15	1.55	-0.17	5.00
Jan 80	1.32	-1.42	1.10	-1.20	-352	4.89	-4.00	12.30
Feb 80	0.63	-3.02	2.57	-4.96	-1454	3.76	-16.50	-3.98
Mar 80	0.77	-1.34	1.89	-2.46	-721	2.49	-8.20	0.10
Apr 80	2.23	0.39	1.11	1.57	460	0.00	5.23	5.25
May 80	3.51	0.04	1.09	2.46	721	0.00	8.20	8.20
Total	22.35	-3.01	14.98	4.36	1277	12.89	14.72	57.69
Average	1.86	-0.25	1.25	0.36	106	1.07	1.23	4.81

*Total Savings Fossil Equivalent = Net Electrical Savings/0.3

**The energy in this column is the amount that would have been saved if the system had operated in the heat pump solar mode instead of the solar plus heat strip mode.

***The total savings in this column is derived by adding the Net Electrical Savings and the energy savings from the Elimination of Solar Plus Heat Strip Mode and dividing the sum by 0.3 where the factor 0.3 accounts for the efficiency in generating and transferring power from the source to the load.

Either of the alternatives is considerably better than the actual savings associated with the space heating subsystem of -3.01 million Btu.

The method utilized to derive space heating savings is described in detail in Appendix D. The month of February, 1980, when the greatest savings loss was incurred is used as an example in the Appendix. The results indicate that the space heating savings loss of -4.96 million Btu might have actually been a savings of 0.86 million Btu if the system had operated as designed. However, this small savings is still low in comparison to the net solar energy savings of 6.22 million Btu that would be achieved if the solar energy is delivered directly to the space heating system (7.57 million Btu less the operating energy of 1.35 million Btu).

In summary, the hot water savings were substantial, but the space heating system actually accrued a loss. Operating the system as designed would have improved the situation. However, the savings would still be lower than anticipated for a system of this type. Utilizing all the solar energy to heat hot water or utilizing the space heating direct mode exclusively would have been considerably more beneficial.

6. MAINTENANCE

A considerable amount of maintenance was required at the Wormser site since activation.

The thermal storage tank was unsealed and thermal transport piping uninsulated until late October, 1978, when the storage tank subsystem was repaired.

The collector subsystem was inoperative until November 2, 1978, when air was bled from the transport piping.

Unit #2 heat pump was repaired between January 3 and 5, 1979 and the apartment occupied shortly thereafter.

The DHW controller failed February 1, 1979, and was not repaired until March 22, 1979.

In June, 1979, the DHW controller set points were adjusted which significantly improved that subsystem's performance.

By July, 1979, all the Townhouse apartments were occupied and the hot water consumption reached high levels.

The space heating solar control system allowed an undesirable solar plus heat strip mode to exist during the winter months. It is believed that this condition resulted from overpressure conditions in the heat pumps and to blown fuses in the control panels. Attempts were made to correct these conditions but the problem reoccurred through the winter season.

7. SUMMARY AND CONCLUSIONS

During the 12 month reporting period, the measured daily average incident insolation in the plane of the collector array was 1,348 Btu/Ft^2. This was eleven percent below the long-term daily average of 1,510 Btu/Ft^2. The measured insolation appears to be an accurate representation of the long-term average for the area. Both the long-term averages for ambient temperature and insolation are derived from data taken at the Columbia South Carolina airport. During the period from June, 1979, through May, 1980, the measured average outdoor ambient temperature was 62°F. This was two degrees below the long-term average of 64°F for the same period. As a result 2,693 heating degree-days were accumulated, as compared to the long-term average of 2,598 heating degree-days.

The solar energy system satisfied 33 percent of the total measured load (hot water plus space heating) during the 12 month reporting period. The space heating solar fraction for the reporting period was 42 percent. However, the computations do not account for uncontrolled losses of solar energy into the building that result primarily from transport piping losses. As discussed in Section 3.2.4, these losses are substantial and provide a considerable reduction in the measured space heating load.

A total of 568.00 million Btu of incident solar energy was measured in the plane of the collector array during the reporting period. The system collected 72.35 million Btu of the available energy, which represents a collector array efficiency of 13 percent. During periods when the collector array was active, a total of 484.97 million Btu was measured in the plane of the collector array. Therefore, the operational collector efficiency was 15 percent. These collector efficiencies are referenced to the solar window area per National Bureau of Standards Procedures. However, if the collector efficiencies are referenced to the collector absorber area, which is the normal evaluation procedure, the indicated collector aray efficiency is 56 percent and the operational collector array efficiency is 65 percent. If the multiplication effect is removed and the resultant efficiency referenced to absorber area, then collector efficiency is 0.31 and the operational collector efficiency is 0.36. These latter collector efficiency indications indicate that the collector array is performing well.

During the reporting period, a total of 69.42 million Btu of solar energy was delivered to the storage tanks. During this same time period 46.98 million Btu were removed from storage for support of the domestic hot water and space heating loads. The majority of this (27.45 million Btu) went to the space heating subsystem and the remainder was used in support of the domestic hot water subsystem. The effective storage heat loss coefficient was 95.5 Btu/Hr-°F, which is about normal and indicates a suitable insulated storage subsystem. The average temperature of storage was 101°F for the period.

The hot water load for the 12 month reporting period was 62.88 million Btu. A total of 22.46 million Btu of solar energy and 62.28 million Btu of auxiliary energy were supplied to the subsystem, which represents a weighted hot water solar fraction of 23 percent. The average daily consumption of hot water was 254 gallons, delivered at an average temperature of 151°F. A total of 21.86 million Btu was lost from the hot water tank during the reporting period. This large loss is due to the high domestic hot water consumption, large heat loss coefficient associated with domestic hot water storage tank and large thermal transport piping losses.

The measured space heating load was 65.04 million Btu for the reporting period. The heating solar fraction for the 12 month period was 42 percent During the reporting period, a total of 27.45 million Btu of measured solar energy and 27.01 million Btu of auxiliary thermal energy were delivered to the space heating load, and this energy maintained an average building temperature of 73°F. The 27.01 million Btu of auxiliary thermal energy supplied to the space heating subsystem represents 31.59 million Btu, or 9256 kWh of electricity that were required for support of the space heating load.

A total of 14.98 million Btu, or 4389 kWh, of electrical operating energy was required to support the solar energy system during the 12 month reporting period. This does not include the electrical energy required to operate the fan in the auxiliary furnace. This fan would be required for operation of the space heating subsystem regardless of the presence of the solar energy system.

The gross electrical savings for the 12 month reporting period were 19.34 million Btu of electrical energy (5667 kWh). However, when the 14.98 million Btu of electrical operating energy is taken into account, the net electrical savings were 4.36 million Btu or 1277 kWh. If a 30 percent efficiency is assumed for power generation and distribution, then the net electrical energy savings translate into a savings of 14.72 million Btu in generating station fuel requirements. This is equivalent to 2.5 barrels of oil. It should also be noted that the fossil energy savings are based only on the measured amount of solar energy delivered to the space heating subsystem. As discussed in Section 3.2.4, the fossil energy savings will increase considerably if the uncontrolled solar energy input to the building is considered. Also if the undesirable solar plus heat strip mode were eliminated the total electrical savings would have increased from 4.36 million Btu to 17.20 million Btu (5040 kWh) and the savings at the source of energy generation would have been 57.33 million Btu or 9.75 barrels of oil.

In general, the Wormser Solar Energy System performed reasonably well during the reporting time period. The space heating subsystem solar energy met 42 percent of the measured space heating load and the hot water subsystem met 23 percent of the measured hot water demand. The space heating savings were seriously reduced because of operating in a solar plus heat strip mode. The heat pump solar mode was inefficient and a direct solar mode only would have made better use of solar energy. However, it must be again stressed that the measured heating subsystem performance does not include the uncontrolled addition of solar energy to the building. If the uncontrolled losses could have been reduced to an inconsequential level, then the measured system performance would have improved considerably.

8. REFERENCES

1. Manual of Installation, Operation, and Maintenance for Pyramidal Optics Solar System; Wormser Scientific Corporation Publication.
2. NASA/DOE CR-150760, Installation Package for a Domestic Solar Heating and Hot Water System, August 1978.
3. Colt Solar Brochure, Colt, Inc., Energy Systems Division, 71-590 San Jacinto, Rancho Mirage, CA.
4. Wormser, E. M., "Pyramidal Optical Collector System Description and Performance Data on a Unique Solar Energy System Developed by Wormser Scientific Corporation," Solar Engineer, July, 1977, p 30-32.
5. Friedrich Solar Assisted Heat Pump Performance Curves for Model 33 and 42 Dual Source Heat Pumps, Friedrich Air Conditioning Company.
6. E. Streed, etc. al., Thermal Data Requirements and Performance Evaluation Procedures for the National Solar Heating and Cooling Demonstration Program, NBSIR-76-1137, National Bureau of Standards, Washington, August, 1976.
7. J. T. Smok, V. S. Sohoni, J. M. Nash, "Processing of Instrumented Data for the National Solar Heating and Cooling Demonstration Program", Conference on Performance Monitoring Techniques for Evaluation of Solar Heating and Cooling Systems, Washington, D. C., April, 1978.
8. ASHRAE Standard 93-77, Methods of Testing to Determine the Thermal Performance of Solar Collectors, The American Society of Heating Refrigeration and Air Conditioning Engineers, Inc., New York, NY, 1977.
9. ASHRAE Standard 94-77, Methods of Testing Thermal Storage Devices Based on Thermal Performance, The American Society of Heating Refrigeration and Air Conditioning Engineers, Inc., New York, NY 1977.
10. McCumber, W. H. Jr., "Collector Array Performance for Instrumented Sites of the National Solar Heating and Cooling Demonstration Program," published and distributed at the 1979 Solar Update Conference.
11. Beckman, William A.; Klein, Sanford A; Duffie, John A.; Solar Heating Design by the f-Chart Method, Wiley Interscience New York, NY, 1977.
12. Mirror Enclosures for Double - Exposure Solar Collectors, D. C. Larson, Solar Energy, Vol. 23 pp 512-529.

APPENDIX A
DEFINITION OF PERFORMANCE FACTORS AND SOLAR TERMS
AND
SOLAR TERMS

APPENDIX A
DEFINITION OF PERFORMANCE FACTORS AND SOLAR TERMS

COLLECTOR ARRAY PERFORMANCE

The collector array performance is characterized by the amount of solar energy collected with respect to the energy available to be collected.

- INCIDENT SOLAR ENERGY (SEA) is the total insolation available on the gross collector array area. This is the area of the collector array energy-receiving aperture, including the framework which is an integral part of the collector structure.

- OPERATIONAL INCIDENT ENERGY (SEOP) is the amount of solar energy incident on the collector array during the time that the collector loop is active (attempting to collect energy).

- COLLECTED SOLAR ENERGY (SECA) is the thermal energy removed from the collector array by the energy transport medium.

- COLLECTOR ARRAY EFFICIENCY (CAREF) is the ratio of the energy collected to the total solar energy incident on the collector array. It should be emphasized that this efficiency factor is for the collector array, and available energy includes the energy incident on the array when the collector loop is inactive. This efficiency must not be confused with the more common collector efficiency figures which are determined from instantaneous test data obtained during steady state operation of a single collector unit. These efficiency figures are often provided by collector manufacturers or presented in technical journals to characterize the functional capability of a particular collector design. In general, the collector panel maximum efficiency factor will be significantly higher than the collector array efficiency reported here.

STORAGE PERFORMANCE

The storage performance is characterized by the relationships among the energy delivered to storage, removed from storage, and the subsequent change in the amount of stored energy.

- ENERGY TO STORAGE (STEI) is the amount of energy, both solar and auxiliary, delivered to the primary storage medium.

- ENERGY FROM STORAGE (STEO) is the amount of energy extracted by the load subsystems from the primary storage medium.

- CHANGE IN STORED ENERGY (STECH) is the difference in the estimated stored energy during the specified reporting period, as indicated by the relative temperature of the storage medium (either positive or negative value).

- STORAGE AVERAGE TEMPERATURE (TST) is the mass-weighted average temperature of the primary storage medium.

- STORAGE EFFICIENCY (STEFF) is the ratio of the sum of the energy removed from storage and the change in stored energy to the energy delivered to storage.

ENERGY COLLECTION AND STORAGE SUBSYSTEM

The Energy Collection and Storage Subsystem (ECSS) is composed of the collector array, the primary storage medium, the transport loops between these, and other components in the system design which are necessary to mechanize the collector and storage equipment.

- INCIDENT SOLAR ENERGY (SEA) is the total insolation available on the gross collector array area. This is the area of the collector array energy-receiving aperture, including the framework which is an integral part of the collector structure.

- AMBIENT TEMPERATURE (TA) is the average temperature of the outdoor environment at the site.

- ENERGY TO LOADS (SEL) is the total thermal energy transported from the ECSS to all load subsystems.

- AUXILIARY THERMAL ENERGY TO ECSS (CSAUX) is the total auxiliary supplied to the ECSS, including auxiliary energy added to the storage tank, heating devices on the collectors for freeze-protection, etc.

- ECSS OPERATING ENERGY (CSOPE) is the critical operating energy required to support the ECSS heat transfer loops.

HOT WATER SUBSYSTEM

The hot water subsystem is characterized by a complete accounting of the energy flow to and from the subsystem, as well as an accounting of internal energy. The energy into the subsystem is composed of electrical auxiliary thermal energy, and the operating energy for the subsystem. In addition, the solar energy supplied to the subsystem, along with solar fraction is tabulated. The load of the subsystem is tabulated and used to compute the estimated electrical savings of the subsystem. The load of the subsystem is further identified by tabulating the supply water temperature, and the outlet hot water temperature, and the total hot water consumption.

- HOT WATER LOAD (HWL) is the amount of energy required to heat the amount of hot water demanded at the site from the incoming temperature to the desired outlet temperature.

- SOLAR FRACTION OF LOAD (HWSFR) is the percentage of the load demand which is supported by solar energy.

- SOLAR ENERGY USED (HWSE) is the amount of solar energy supplied to the hot water subsystem.

- OPERATING ENERGY (HWOPE) is the amount of electrical energy required to support the subsystem, (e.g., fans, pumps, etc.) and which is not intended to affect directly the thermal state of the subsystem.

- AUXILIARY THERMAL USED (HWAT) is the amount of energy supplied to the major components of the subsystem in the form of thermal energy in a heat transfer fluid, or its equivalent. This term also includes the converted electrical and fossil fuel energy supplied to the subsystem.

- AUXILIARY ELECTRICAL FUEL (HWAE) is the amount of electrical energy supplied directly to the subsystem.

- ELECTRICAL ENERGY SAVINGS (HWSVE) is the estimated difference between the electrical energy requirements of an alternative conventional system (carrying the full load) and the actual electrical energy required by the subsystem.

- SUPPLY WATER TEMPERATURE (TSW) is the average inlet temperature of the water supplied to the subsystem.

- AVERAGE HOT WATER TEMPERATURE (THW) is the average temperature of the outlet water as it is supplied from the subsystem to the load.

- HOT WATER USED (HWCSM) is the volume of water used.

SPACE HEATING SUBSYSTEM

The space heating subsystem is characterized by performance factors accounting for the complete energy flow to and from the subsystem. The average building temperature and the average ambient temperature are tabulated to indicate the relative performance of the subsystem in satisfying the space heating load and in controlling the temperature of the conditioned space.

- SPACE HEATING LOAD (HL) is the sensible energy added to the air in the building.

- SOLAR FRACTION OF LOAD (HSFR) is the fraction of the sensible energy added to the air in the building derived from the solar energy system.

- SOLAR ENERGY USED (HSE) is the amount of solar energy supplied to the space heating subsystem.

- OPERATING ENERGY (HOPE) is the amount of electrical energy required to support the subsystem, (e.g., fans, pumps, etc.) and which is not intended to affect directly the thermal state of the subsystem.

- AUXILIARY THERMAL USED (HAT) is the amount of energy supplied to the major components of the subsystem in the form of thermal energy in a heat transfer fluid or its equivalent. This term also includes the converted electrical and fossil fuel energy supplied to the subsystem.

- AUXILIARY FOSSIL FUEL(HAF) is the amount of fossil energy supplied directly to the subsystem.

- FOSSIL ENERGY SAVINGS (HSVF) is the estimated difference between the fossil energy requirements of an alternative conventional system (carrying the full load) and the actual fossil energy required by the subsystem.

- ELECTRICAL ENERGY SAVINGS (HSVE) is the cost of the operating energy (HOPE) required to support the solar energy portion of the space heating subsystem.

- BUILDING TEMPERATURE (TB) is the average heated space dry bulb temperature.

- AMBIENT TEMPERATURE (TA) is the average ambient dry bulb temperature at the site.

ENVIRONMENTAL SUMMARY

The environmental summary is a collection of the weather data which is generally instrumented at each site in the Development Program. It is tabulated in this report for two purposes (1) as a measure of the conditions prevalent during the operation of the system at the site, and (2) as a historical record of weather data for the vicinity of the site.

- TOTAL INSOLATION (SE) is the accumulated total solar energy incident upon the gross collector array measured at the site.

- AMBIENT TEMPERATURE (TA) is the average temperature of the environment at the site.

- DAYTIME AMBIENT TEMPERATURE (TDA is the temperature during the period from three hours before solar noon to three hours after solar noon.

APPENDIX B

SOLAR ENERGY SYSTEM PERFORMANCE EQUATIONS

WORMSER

APPENDIX B

SOLAR ENERGY SYSTEM PERFORMANCE EQUATIONS FOR WORMSER

I. INTRODUCTION

Solar energy system performance is evaluated by performing energy balance calculations on the system and its major subsystems. These calculations are based on physical measurement data taken from each subsystem every 320 seconds. This data is then numerically combined to determine the hourly, daily, and monthly performance of the system. This appendix describes the general computational methods and the specific energy balance equations used for this evaluation.

Data samples from the system measurements are numerically integrated to provide discrete approximations of the continuous functions which characterize the system's dynamic behavior. This numerical integration is performed by summation of the product of the measured rate of the appropriate performance parameters and the sampling interval over the total time period of interest.

There are several general forms of numerical integration equations which are applied to each site. Examples of these general forms are as follows: The total solar energy available to the collector array is given by

$$\text{SOLAR ENERGY AVAILABLE} = (1/60)\ \Sigma\ [\text{I001} \times \text{AREA}] \times \Delta\tau$$

where I001 is the solar radiation measurement provided by the pyranometer in Btu/ft^2-hr, AREA is the area of the collector array in square feet, $\Delta\tau$ is the sampling interval in minutes, and the factor (1/60) is included to correct the solar radiation "rate" to the proper units of time.

Similarly, the energy flow within a system is given typically by

$$\text{COLLECTED SOLAR ENERGY} = \Sigma\ [M100 \times \Delta H] \times \Delta\tau$$

where M100 is the mass flow rate of the heat transfer fluid in lb_m/min and ΔH is the enthalpy change, in Btu/lb_m, of the fluid as it passes through the heat exchanging component.

For a liquid system ΔH is generally given by

$$\Delta H = \bar{C}_p\ \Delta T$$

where $\bar{C}_p$ is the average specific heat, in Btu/(lb_m-°F), of the heat transfer fluid and ΔT, in °F, is the temperature differential across the heat exchanging component.

For an air system ΔH is generally given by

$$\Delta H = H_a(T_{out}) - H_a(T_{in})$$

where $H_a(T)$ is the enthalpy, in Btu/lb_m, of the transport air evaluated at the inlet and outlet temperatures of the heat exchanging component.

$H_a(T)$ can have various forms, depending on whether or not the humidity ratio of the transport air remains constant as it passes through the heat exchanging component.

For electrical power, a general example is

$$\text{ECSS OPERATING ENERGY} = (3413/60)\ \Sigma\ [EP100] \times \Delta\tau$$

where EP100 is the measured power required by electrical equipment in kilowatts and the two factors (1/60) and 3413 correct the data to Btu/min.

These equations are comparable to those specified in "Thermal Data Requirements and Performance Evaluation Procedures for the National Solar Heating and Cooling Demonstration Program." This document, given in the list of references, was prepared by an inter-agency committee of the government, and presents guidelines for thermal performance evaluation.

Performance factors are computed for each hour of the day. Each numerical integration process, therefore, is performed over a period of one hour. Since long-term performance data is desired, it is necessary to build these hourly performance factors to daily values. This is accomplished, for energy parameters, by summing the 24 hourly values. For temperatures, the hourly values are averaged. Certain special factors, such as efficiencies, require appropriate handling to properly weight each hourly sample for the daily value computation. Similar procedures are required to convert daily values to monthly values.

II. PERFORMANCE EQUATIONS

The performance equations for Wormser used for the data evaluation of this report are contained in the following pages and have been included for technical reference and information.

EQUATIONS USED IN MONTHLY PERFORMANCE ASSESSMENT

NOTE: MEASUREMENT NUMBERS REFERENCE SYSTEM SCHEMATIC FIGURE 2-1

AVERAGE AMBIENT TEMPERATURE (°F)

$$TA = (1/60) \times \Sigma\ T001 \times \Delta\tau$$

AVERAGE BUILDING TEMPERATURE (°F)

$$TB = (1/60) \times \Sigma\ (T601 + T602 + T603 + T604)/240 \times \Delta\tau$$

DAYTIME AVERAGE AMBIENT TEMPERATURE (°F)

$$TDA = (1/360) \times \Sigma\ T001 \times \Delta\tau$$

FOR $\pm$3 HOURS FROM SOLAR NOON

INCIDENT SOLAR ENERGY PER SQUARE FOOT (BTU/FT^2)

$$SE = (1/60) \times \Sigma\ I001 \times \Delta\tau$$

OPERATIONAL INCIDENT SOLAR ENERGY (BTU)

$$SEOP = (1/60) \times \Sigma\ [I001 \times CLAREA] \times \Delta\tau$$

WHEN THE COLLECTOR LOOP IS ACTIVE

SOLAR ENERGY COLLECTED BY THE ARRAY (BTU)

$$SECA = \Sigma\ [M101 \times HWD\ (T151, T101)] \times \Delta\tau$$

ENTHALPY FUNCTION FOR WATER (BTU/LBM)

$$HWD(T_2,T_1) = \int_{T_1}^{T_2} C_p(T)dT$$

THIS FUNCTION COMPUTES THE ENTHALPY CHANGE OF WATER AS IT PASSES THROUGH A HEAT EXCHANGING DEVICE.

SOLAR ENERGY TO SPACE HEATING (BTU)

$$CSE01 = \Sigma [M401 \times HWD (T451, T401)] \times \Delta\tau$$

SOLAR ENERGY TO STORAGE (BTU)

$$STEI = SECA - CSE01 \text{ IF } SECA > CSE01$$

SOLAR ENERGY FROM STORAGE TO SPACE HEATING (BTU)

$$STE01 = CSE01 - SECA \text{ IF } CSE01 > SECA$$

SOLAR ENERGY FROM STORAGE TO HOT WATER (BTU)

$$STE02 = \Sigma [M305 \times HWD (T305, T355)] \times \Delta\tau$$

SOLAR ENERGY TO LOADS (BTU)

$$STE0 = STE01 + STE02$$

SOLAR ENERGY TO SPACE HEATING

$$HSE1 = CSE01$$

SOLAR ENERGY FROM STORAGE (BTU)

$$STE0 = STE01 + STE02$$

AVERAGE TEMPERATURE OF STORAGE (°F)

$$TSTM = \Sigma [(T201 + T202 + T203)/3] \times \Delta\tau$$

$$TSTL = TSTM$$

$$TST = (1/60) \times TSTM$$

ENERGY DELIVERED FROM ECSS TO-LOAD SUBSYSTEMS (BTU)

$$CSE0 = CSE01 + STE02$$

ECSS OPERATING ENERGY (BTU)

$$CSOPE = 56.8833 \times \Sigma EP101 \times \Delta\tau$$

SPACE HEATING SUBSYSTEM SOLAR OPERATING ENERGY (BTU)

$$HOPE2 = 56.8833 \times \Sigma EP405 \times \Delta\tau$$

HOT WATER CONSUMED (GALLONS)

$HWCSM = \Sigma\ (WD301 + WD302 + WD303 + WD304) \times \Delta\tau$

HOT WATER LOAD (BTU)

$HWL = \Sigma\ \{[M301 \times HWD\ (T351, T301)] + [M302 \times HWD\ (T352, T302)] + [M303 \times HWD\ (T353, T303)] + [M304 \times HWD\ (T354, T304)]\} \times \Delta\tau$

SOLAR ENERGY TO HOT WATER SUBSYSTEM (BTU)

$HWSE = CSE02$

HOT WATER SUBSYSTEM AUXILIARY ELECTRICAL FUEL ENERGY (BTU)

$HWAE = 56.8833 \times \Sigma\ (EP302 + EP303 + EP304 + EP305) \times \Delta\tau$

HOT WATER SUBSYSTEM OPERATING ENERGY (BTU)

$HWOPE = 56.8833 \times \Sigma\ EP301 \times \Delta\tau$

SOLAR ENERGY TO SPACE HEATING SUBSYSTEM (BTU)

$HSE = CSE01$

SPACE HEATING CIRCULATING FAN ENERGY (BTU)

$HOPEA = 56.8833 \times \Sigma\ (EP405 + HOPE11) \times \Delta\tau$

WHERE HOPE11 IS CIRCULATING FAN ENERGY DERIVED FROM EP401, EP402, EP403, AND EP404

SPACE HEATING SUBSYSTEM OPERATING ENERGY (BTU)

$HOPE = HOPEA + HOPE2$

SUPPLY WATER TEMPERATURE (°F)

$TST = (T301 + T302 + T303 + T304)/4$

HOT WATER TEMPERATURE (°F)

$THW = (T351 + T352 + T353 + T354)/4$

BOTH TSW AND THW ARE COMPUTED ONLY WHEN FLOW EXISTS IN THE SUBSYSTEM, OTHERWISE THEY ARE SET EQUAL TO THE VALUES OBTAINED DURING THE PREVIOUS FLOW PERIOD.

INCIDENT SOLAR ENERGY ON COLLECTOR ARRAY (BTU)

SEA = CLAREA x SE

COLLECTED SOLAR ENERGY (BTU/FT^2)

SEC = SECA/CLAREA

COLLECTOR ARRAY EFFICIENCY

CAREF = SECA/SEA

CHANGE IN STORED ENERGY (BTU)

STECH1 = STOCAP x TSTL x CP (TSTL) x RHO (TSTL)

STECH = STECH1 - STECH 1_p

WHERE THE SUBSCRIPT $_p$ REFERS TO A PRIOR REFERENCE VALUE

STORAGE EFFICIENCY

STEFF = (STECH + STEO)/STEI

SOLAR ENERGY TO LOAD SUBSYSTEMS (BTU)

SEL = HSE + HWSE

ECSS SOLAR CONVERSION EFFICIENCY

CSCEF = SEL/SEA

HEATING AUXILIARY ENERGY (BTU)

HAE = HAE1 + HAE2

AUXILIARY THERMAL ENERGY TO HOT WATER SUBSYSTEM (BTU)

HWAT = HWAE

HOT WATER SOLAR FRACTION (PERCENT)

HWSFR = 100 x HWTKSE/(HWTKSE + HWTKAUX)

WHERE HWTKSE AND HWTKAUX REPRESENT THE CURRENT SOLAR AND AUXILIARY ENERGY CONTENT OF THE HOT WATER TANK

HOT WATER ELECTRICAL ENERGY SAVINGS (BTU)

HWSVE = HWSE - HWOPE

SPACE HEATING LOAD (BTU)

IF TIME $\leq$ OCTOBER 1, 1979

HL = HLT + HAE2 + CSE01

IF TIME > OCTOBER 1, 1979

IF EP405 > 0

HL = HAT + CSE01

IF EP405 $\leq$ 0

HL = HAE1X x HPCOPIA + HAE2 + CSE01

SPACE HEATING SUBSYSTEM SOLAR FRACTION (PERCENT)

HSFR = 100 x HSE/HL

SPACE HEATING SUBSYSTEM ELECTRICAL ENERGY SAVINGS (BTU)

HSVE = [(HPFRAC x HL/HPCOP1A + (1-HPFRAC) x HL)

-(HAE1 + HAE2 + HOPE2)]

SYSTEM LOAD (BTU)

SYSL = HL + HWL

SOLAR FRACTION OF SYSTEM LOAD (PERCENT)

SFR = (HL x HSFR + HWL x HWSFR)/SYSL

SYSTEM OPERATING ENERGY (BTU)

SYSOPE = CSOPE + HWOPE + HOPE

AUXILIARY THERMAL ENERGY TO LOADS (BTU)

AXT = HWAT + HAT

AUXILIARY ELECTRICAL ENERGY TO LOADS (BTU)

AXE = HWAE + HAE

TOTAL ELECTRICAL ENERGY SAVINGS (BTU)

TSVE = HWSVE + HSVE - CSOPE

TOTAL ENERGY CONSUMED (BTU)

TECSM = SYSOPE + AXE + AXF + SECA

SYSTEM PERFORMANCE FACTOR

SYSPF = SYSL/(AXF + (AXE + SYSOPE) x 3.33)

COOLING LOAD FOR INFORMATION ONLY (BTU)

IF T001 > 65/EP405 = 0

CL = 56.8833 x Σ [(EP401 + EP402 + EP403 + EP404) x HPCOOL] x $\Delta\tau$

OVERALL HEAT PUMP PERFORMANCE (BTU)

TCEL = HL

TCEI = HAE1 + HOPE2 + HAE2

TCEOP = TCEL/TCEI

HEAT PUMP COP CALCULATIONS

T451 < 40

HPCOP1 = 2.16

HT451 > 40

HPCOP1 = 2.16 + 0.0175 x (T451 - 40)

T451 < 40

HPCOP2 = HPCOP3 = 1.75

T451 > 40

HPCOP2 = HPCOP3 = 1.75 + 0.027 x (T451 - 40)

T451< 40

HPCOP4 = 2.13

T451 > 40

HPCOP4 = 2.13 + 0.017333 x (T451 - 40)

HPFRAC & CAPN CALCULATION

T001 > -10 & T001 < 40

CAPN = 0.473 + T001 x 0.0104

T001 > 40

CAPN = 0.889 + (T001 - 40) x 0.01934

TEMP = (T601 + T602 + T603 + T604)/4

T001 < 20

HPFRAC = 0

T001 > 30

HPFRAC = 1

T001 > 20 & T001 < 30

HPFRAC = 1.3 x CAPN x (TEMP - 28)/(TEMP - T001)

HAE3

T001 < 65 & TIME < OCTOBER 1, 1979

HAE3 = 56.8833 + Σ (EP401 + EP402 + EP403 + EP404
-HOPE11) x $\Delta\tau$

T001 < 65 & TIME > OCTOBER 1, 1979

HAE3 = 56.8833 + Σ (EP411 + EP412 + EP413 + EP414) x $\Delta\tau$

CALCULATE ESTIMATED HEAT PUMP POWER INPUT

HP42 = 3.3 + T001 x 0.03167

HP33 = 2.6 + T001 x 0.025

HP33L = 1.925 + T451 x 0.01875

HP42L = 2.434 + T451 x 0.023864

HAE1 CALCULATION

TIME < OCTOBER 1, 1979

EP405 > 0 & T451 < 82 & T001 < 65

HAE1 = 0 & SUMHP = 0

EP401 > 0.8 & EP401 < HP42L + .5

HAE1 = 56.8833 x Σ [(EP401 - 0.75)] x Δτ + HAE1

EP402 > 0.8 & EP402 < HP33L + .3

HAE1 = 56.8833 x Σ (EP402) x Δτ + HAE1

EP403 > 0.8 & EP403 < HP33L + .3

HAF1 = 56.8833 x Σ (EP403) x Δτ x HAE1

EP404 > 0.8 & EP404 < HP42L + .5

HAE1 = 56.8833 x Σ [(EP404 - .7)] x Δτ + HAE1

EP405 > 0 T451 < 82 & T001 < 65

EP401 ≥ HP42L + .5

SUMHP = -HP42L + SUMHP + EP401

HAE1 = HAE1 + 56.8833 Σ [(HP42L - .75)] x Δτ

EP402 > HP33L + .3

SUMHP = - HP33L + SUMHP + EP402

HAE1 = HAE1 + 56.8833 Σ (HP33L - .38) x Δτ

EP403 ≥ HP33L + .3

SUMHP = -HP33L + SUMHP + EP403

HAE1 = HAE1 + 56.8833 Σ HP33L - .37) x Δτ

EP404 ≥ HP42L + .5

SUMHP = -HP42L + SUMHP + EP404

HAE1 = HAE1 + 56.8833 Σ (HP42L - .70) x Δτ

EP405 = 0 T001 < 65 & T001 > 20

EP401 > HP42 - .2 & EP401 < HP42 + .2

HLT = 56.8833 x Σ (HPCOPIA x EP401) x Δτ

HAE1 = HAE1 + 56.8833 x Σ (EP401 - .75) x Δτ

EP402 > HP33 - .82 & EP402 < HP33

HLT2 = 56.8833 x Σ (EP402 + .38) x Δτ

HAE1 = HAE1 + 56.8833 x Σ EP402 x Δτ

EP403 > HP33 - .78 & EP403 < HP33

HLT3 = 56.8833 x Σ (EP403 + .37) x Δτ

HAE1 = HAE1 + 56.8833 x Σ EP403 x Δτ

EP404 > HP42 - .2 & EP404 < HP42 + .2

HLT4 = 56.8833 x Σ (EP404) x Δτ

HAE1 = HAE1 + 56.8833 x Σ (EP404 - .7) x Δτ

EP405 = 0 T001 < 65 T001 > 20

EP401 $\geq$ HP42 + .2 & EP401 > 9.6

HLT = 56.8833 x Σ (HPCOPIA XHP42) x Δτ

SUMP = SUMHP - Σ (HP42 + EP401) x Δτ

HAE1 = HAE1 + 56.8833 x Σ (HP42 - .75) x Δτ

EP402 $\geq$ HP33 & EP402 < 9.6

HLT2 = 56.8833 x Σ (HPCOP2A x HP33) x Δτ

SUMHP = SUMHP - Σ (HP33 + EP402) x Δτ

HAE1 = HAE1 + 56.8833 x Σ (HP33 - .38) x Δτ

EP403 $\geq$ HP33 & EP402 < 9.6

HLT3 = 56.8833 x Σ (HPCOP3A x HP33) x Δτ

SUMHP = SUMHP - Σ (HP33 + EP403) x Δτ

HAE1 = HAE1 + 56.8833 x Σ (HP33 - .37) x Δτ

EP404 > HP42 & EP404 < 9.6

HLT = 56.8833 x Σ (HPCOP3A x HP42) x $\Delta\tau$

SUMHP = SUMHP - Σ (HP42 + EP404) x $\Delta\tau$

HAE1 = HAE1 + 56.8833 x Σ (HP42 - .7) x $\Delta\tau$

HLT = HLT1 + HLT2 + HLT3 + HLT4

TIME > OCTOBER 1, 1979

TOO1 < 65

HAE1 = 0

EP405 > 0

EP401 > .8

HAE1 = HAE1 + 56.8833 x Σ (EP401 - .75) x $\Delta\tau$

EP402 > .5

HAE1 = HAE1 + 56.8833 x Σ (EP402) x $\Delta\tau$

EP403 > .5

HAE1 = HAE1 + 56.8833 x Σ (EP403) x $\Delta\tau$

EP403 > .8

HAE1 = HAE1 + 56.8833 x Σ (EP404 - .7) x $\Delta\tau$

EP405 $\leq$ 0

EP401 > HP42 - 0.1

HAE1 = HAE1 + 56.8833 x Σ (EP401 - .75) x $\Delta\tau$

EP402 > HP33 - .52

HAE1 = HAE1 + 56.8833 x Σ EP402 x $\Delta\tau$

EP403 > HP33 - .48

HAE1 = HAE1 + 56.8833 x Σ EP403 x $\Delta\tau$

EP404 > HP42 - 0.1

HAE1 = HAE1 + 56.8833 x Σ (EP401 - .7) x $\Delta\tau$

HAE1X CALCULATION

IF TIME > OCTOBER 1, 1979

T001 < 65

HAE1X = 0

FP405 > 0

EP401 > .8

$$HAE1X = HAE1X + 56.8833 \times \Sigma (HPCOP1 \times EP401) \times \Delta\tau$$

EP402 > .5

$$HAE1X = HAE1X + 56.8833 \times \Sigma [HPCOP2 \times (EP402 + .38)] \times \Delta\tau$$

EP403 > .5

$$HAE1X = HAE1X + 56.8833 \times \Sigma [HPCOP3 \times (EP403 + .37)] \times \Delta\tau$$

EP404 > .5

$$HAE1X = HAE1X + 56.8833 \times \Sigma (HPCOP4 \times EP404) \times \Delta\tau$$

EP405 $\leq$ 0

EP401 > HP42 - .1

$$HAE1X = HAE1X + 56.8833 \Sigma (EP401) \times \Delta\tau$$

EP402 > HP33 - 0.52

$$HAE1X = HAE1X + 56.8833 \times \Sigma (EP402 + .38) \times \Delta\tau$$

EP403 > HP33 - 0.48

$$HAE1X = HAE1X + 56.8833 \times \Sigma (EP403 + .37) \times \Delta\tau$$

ED404 > HP42 - .1

$$HAE1X = HAE1X + 56.8833 \times \Sigma (EP404) \times \Delta\tau$$

HAE2 CALCULATION

TIME < OCTOBER 1, 1979

HLT > 0

HAE2 = SUMHP

HLT $\leq$ 0

HAE2 = HAE3

TIME > OCTOBER 1, 1979

HAE2 = HAE3

HLT = 0

TFI CALCULATION

$TFI = \Sigma\ (T101)/60 \times \Delta\tau$

FLDFLW CALCULATION

$FLDFLW = \Sigma\ M101 \times \Delta\tau$

UNIT 4 SAVINGS CALCULATION

EP405 > 0 & EP404 > 0 & EP404 < .8

$SAV4 = 56.8833 \times \Sigma\ [EP414\ (1 - \frac{1}{HPCOPT})] \times \Delta\tau$

UNIT 3 SAVINGS CALCULATION

EP405 > 0 & EP403 > 0 & EP403 < .5

$SAV3 = 56.8833 \times \Sigma\ EP413\ (1 - \frac{1}{HPCOPT}) \times \Delta\tau$

UNIT 2 SAVING CALCULATION

EP405 > 0 & EP402 > 0 & EP402 < .5

$SAV2 = 56.8833 \times \Sigma\ EP412\ (1 - \frac{1}{HPCOPT}) \times \Delta\tau$

APPENDIX C

LONG-TERM AVERAGE WEATHER CONDITIONS

APPENDIX C

LONG-TERM AVERAGE WEATHER CONDITIONS

The environmental estimates given in this appendix provide a point of reference for evaluation of weather conditions as reported in the Monthly Performance Assessments and Solar Energy System Performance Evaluations issued by the National Solar Data Program. As such, the information presented can be useful in prediction of long-term system performance.

Environmental estimates for this site include the following monthly averages: extraterrestrial insolation, insolation on a horizontal plane at the site, insolation in the tilt plane of the collection surface, ambient temperature, heating degree-days, and cooling degree-days. Estimation procedures and data sources are detailed in the following paragraphs.

The preferred source of long-term temperature and insolation data is "Input Data for Solar Systems" (IDSS) [1] since this has been recognized as the solar standard. The IDSS data are used whenever possible in these environmental estimates for both insolation and temperature related sources; however, a secondary source used for insolation data is the Climatic Atlas of the United States [2], and for temperature related data, the secondary source is "Local Climatological Data" [3].

Since the available long-term insolation data are only given for a horizontal surface, solar collection subsystem orientation information is used in an algorithm [4] to calculate the insolation expected in the tilt plane of the collector. This calculation is made using a ground reflectance of 0.2.

REFERENCES

[1] Cinquemani, V., et al. "Input Data for Solar Systems." Prepared for the U.S. Department of Energy by the National Climatic Center, Asheville, NC, 1978.

[2] United States Department of Commerce, Climatic Atlas of the United States, Environmental Data Service, Reprinted by the National Oceanic and Atmospheric Administration, Washington, DC, 1977.

[3] United States Department of Commerce, "Local Climatological Data," Environmental Data Service, National Oceanic and Atmospheric Administration, Asheville, NC, 1977.

[4] Klein, S. A., "Calculation of Monthly Average Insolation on Tilted Surfaces," Joint Conference 1976 of the International Solar Energy Society and the Solar Energy Society of Canada, Inc., Winnipeg, August 15-20, 1976.

SITE: WORMSER 45. LOCATION: COLUMBIA SC

ANALYST: K. SHENFISH DRIVE NO.: 7.

COLLECTOR TILT: 27.00 (DEGREES) COLLECTOR AZIMUTH: 0.0 (DEGREES)

LATITUDE: 33.95 (DEGREES) RUN DATE: 04/29/80

MONTH	HOBAR	HBAR	KBAR	RBAR	SBAR	HDD	CDD	TBAR
JAN	1649.	763.	0.46294	1.420	1084.	608	0	45.
FEB	2084.	1021.	0.49010	1.286	1313.	493	5	48.
MAR	2621.	1357.	0.51776	1.147	1556.	360	25	54.
APR	3146.	1748.	0.55559	1.023	1789.	83	56	64.
MAY	3488.	1895.	0.54327	0.940	1781.	12	233	72.
JUN	3618.	1947.	0.53813	0.906	1763.	0	414	79.
JUL	3545.	1844.	0.52009	0.921	1698.	0	502	81.
AUG	3270.	1703.	0.52089	0.984	1677.	0	471	80.
SEP	2805.	1438.	0.51269	1.092	1570.	0	289	75.
OCT	2237.	1213.	0.54224	1.253	1520.	112	87	64.
NOV	1748.	922.	0.52723	1.416	1305.	341	5	54.
DEC	1525.	723.	0.47372	1.477	1068.	589	0	46.

LEGEND:

HOBAR ==> MONTHLY AVERAGE DAILY EXTRATERRESTRIAL RADIATION (IDEAL) IN BTU/DAY-FT2.

HBAR ==> MONTHLY AVERAGE DAILY RADIATION (ACTUAL) IN BTU/DAY-FT2.

KBAR ==> RATIO OF HBAR TO HOBAR.

RBAR ==> RATIO OF MONTHLY AVERAGE DAILY RADIATION ON TILTED SURFACE TO THAT ON A HORIZONTAL SURFACE FOR EACH MONTH (I.E., MULTIPLIER OBTAINED BY TILTING).

SBAR ==> MONTHLY AVERAGE DAILY RADIATION ON A TILTED SURFACE (I.E., RBAR * HBAR) IN BTU/DAY-FT2.

HDD ==> NUMBER OF HEATING DEGREE DAYS PER MONTH.

CDD ==> NUMBER OF COOLING DEGREE DAYS PER MONTH.

TBAR ==> AVERAGE AMBIENT TEMPERATURE IN DEGREES FAHRENHEIT.

APPENDIX D

WORMSER SPACE HEATING SAVINGS ANALYSIS

FOR THE MONTH OF FEBRUARY

The savings in electrical energy by a solar energy system for which a heat pump is the conventional source is

$$(1) \qquad HSVE = \left[\begin{array}{l}\text{Electrical Energy Expenditures} \\ \text{for Heat Pump System}\end{array}\right]_c - \left[\begin{array}{l}\text{Electrical Energy Expenditures} \\ \text{for Solar Heating System} \\ \text{(including auxiliary)}\end{array}\right]_s$$

where c denotes conventional heating system
s denotes solar heating system

Thus to compute savings in energy for a heat pump-referenced solar system, the expenditure in energy must be first determined assuming no solar exists. To do this for a conventional heat pump system, you cannot simply divide the heating load by the COP, since for a properly designed heat pump system, strip heat will contribute part of the total energy required for some periods of operation, and the coefficient of performance (COP) is different for resistance heating.

With this in mind, the savings equation may be rewritten

$$(2) \qquad HSVE = \left[\frac{HPFRAC * HL}{HPCOPH} + \frac{(1\text{-}HPFRAC) * HL}{COPSTRIP}\right]_c$$

$$- \left[\begin{array}{l}\text{Measured Total} \\ \text{Heat Pump} \\ \text{Input}\end{array}\right] + \left[\begin{array}{l}\text{Measured} \\ \text{Strip Heat} \\ \text{Input}\end{array}\right] + \left[\begin{array}{l}\text{Operating} \\ \text{Energy}\end{array}\right]_s$$

Where HPFRAC = The fraction of the heating load HL that is met by the heat pump

HPCOPH = The COP of the heat pump. As defined here HPCOPH is the ratio of the output heating capacity of the heat pump to total electrical input, <u>including</u> the power required for the evaporator fan and air distribution blower

COPSTRIP = The COP of the strip heaters (assumed to be 1.0)

What is required is a method of determing the fraction of the total load that will be provided by the heat pump (HPFRAC), and knowledge of the heat pump COP (HPCOPH).

The Wormser solar heat pump COP is computed from curve fits to the manufacturers performance specifications for the specially designed multi-mode Friedrich heat pumps utilized in the Wormser solar energy system. The HPCOPH are functions of energy sources inlet temperatures, i.e., (HPCOPH1 = 2.16 + 0.0175* (T451-40), where T451 is temperature of inlet water to unit number 1 heat pump).

The ambient temperature where the capacity of the heat pumps just meet the heating load of the condominium units is called the balance point (See figure)

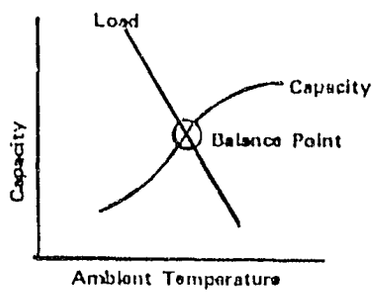

At ambient temperature below the balance point, supplemental heating will be required and this is provided by the strip heaters. The balance point for the Friedrich heat pumps in conjunction with the Wormser unit heating loads is about 30°F. Above 30°F, all heating energy is provided by the heat pump; below 30°F, part of the energy will be supplied by the heat pump and part by electrical heat strips. Below 20°F, the system was designed to utilize heat strips only. The heat pump is capable of performing below 20°F, however, high pressure conditions of this heat pump configuration require the switch to heat stirps.

Since the output (capacity) of a heat pump varies with the outside ambient temperature (TA), obviously HPFRAC will as well. Let CAP(TA) represent the heat pump capacity as a function of ambient temperature.

Then $$HPFRAC = \frac{CAP(TA)}{HL}$$

$$= \frac{CAP(TA)}{UA(TB-TA)}$$

where UA = overall conductance of structure between inside building temperature and outside ambient temperature

TB = building inside temperature

Utilizing the approach developed above HPFRAC is calculated as follows:

HPFRAC = 1.0 $TA \geq 30°F$

HPFRAC = 0 $TA \leq 20°F$

HPFRAC = 1.3 CAPN * (TB)/(TB-TA)

where TB = building temperature

CAPN = 0.473 + T001 * 0.0104 below 40°F

= 0.889 + (T001 -40) * 0.019034 above 40°F

The parameters computed by the performance factor equations with the Wormser savings equation for the month of February are:

HPFRAC = 0.9715

HPCOPH (air to air) = 2.408

Utilizing these parameters the contributions to the space heating load if the control system had been operating properly should have been:

Measured space heating load = 17.40 million Btu

Heat pump/solar = 0.9715 * 17.40 = 16.90 million Btu

Electric Strips = (1 - 0.9715) * 17.40 = 0.50 million Btu

The actual measured space heating subsystem contributions were:

Heat pump/solar = 11.40 million Btu
Electric Strip = 6.0 million Btu

The difference between the expected and actual space heating subsystem contributions is due to operating units 2, 3 and 4 in a solar plus heat strip mode instead of a solar heat pump mode. The effect of operating the space heating subsystem in the solar plus heat strip mode was to increase considerably the amount of electric heat strip operation above and beyond that normally required.

The solar system savings computation for the month of February is as follows:

$$HSVE = \left[\frac{HPFRAC * HL}{HPCOPH\ (AIR\ TO\ AIR)} + (1 - HPFRAC) * HL\right]_c$$

$$- \left[\begin{array}{l}\text{Measured} \\ \text{Heat Pump} \\ \text{Input}\end{array} + \begin{array}{l}\text{Measured} \\ \text{Strip Heat} \\ \text{Input}\end{array} + \begin{array}{l}\text{Solar} \\ \text{Operating} \\ \text{Energy}\end{array}\right]_s$$

$$= \left[\frac{0.9715 * 17.4}{2.408} + (1 - 0.9715) * 17.4\right]_c$$

$$- [5.15 + 6.0 + 1.34]_s$$

$$= [7.02 + 0.50]_c - [5.15 + 6.0 + 1.34]_s$$

$$= 7.52_c - 12.49_s$$

HSVE = -4.96 million Btu

This indicates that conventional space heating during the month would have been superior to operating the solar system as it was.

Now, if the solar system was operated as designed the following conditions probably would have existed:

HL (Actual) = Heat Pump/solar + Direct solar + heat strip + air to air operations
= 17.4

Heat Pump/Solar = 17.4 - 1.37 - 6.0 - .134 * 2.408
= 9.71 million Btu

HPCOPH (Solar) = $\frac{9.71}{5.15}$ = <u>1.88</u>

HL (Probable) = 17.4 million Btu

Total solar required = 9.72 million Btu

The actual heat pump performance was computed to have a COP of 1.88 considerably less than the conventional system performance. The total solar energy requirement would be 9.71 million Btu which is slightly less than the 9.78 million Btu the system collected. Thus, the solar system would have had to operate at a very high efficiency to meet the indicated heating demand while operating as it was designed.

Assuming the solar system could supply the indicated energy requirement, then the actual energy savings would be as follows:

Heat pump electrical requirements =

$$\frac{\text{TOTAL SOLAR REQUIRED - DIRECT SOLAR}}{\text{HPCOP(SOLAR)}} = \frac{9.71 - 1.37}{1.88} = 4.44 \text{ million Btu}$$

HSVE = Conventional requirements - Heat pump electrical requirements
- Strip heat requirements - solar operation requirements

$$= 7.52 - 4.44 - 0.5 - \frac{9.71}{7.57} * 1.34$$

HSVE = 0.86 million Btu

Thus, the solar system operating as design might have provided an actual savings. However, this assumes peak operation of the solar system which is unlikely. For the month of February, the solar system operating as designed would achieve very little savings even though the solar available this month was above average.

☆ U.S. GOVERNMENT PRINTING OFFICE: 1980—640-247/104 REGION NO'4